

RESERVOIR CHARACTERIZATION OF THE “BAWI FIELD”, GREATER UGHELLI DEPOBELT, NIGER DELTA, NIGERIA USING 3-D ATTRIBUTES ASSISTED SEISMIC INTERPRETATION

A. I. Opara^{1*}, S. A. Chukwu¹, S.O.Onyekuru, A. C. Ekwe², C. N. Okereke¹, U. O. Anyiam¹, I. O. Njoku¹, H. N. Echetama¹

¹ Department of Geosciences, Federal University of Technology, PMB 1526, Owerri, Imo State, Nigeria

² Department of Geology/ Geophysics, Federal University Ndufu-Alike Ikwo, Abakaliki Nigeria

³ Department of Geology, Oklahoma State University, United States of America

Received April 1, 2018; Accepted June 20, 2018

Abstract

Seismic interpretation of the “Bawi Field”, Greater Ughelli Depobelt Niger Delta Nigeria was carried out with the objective of characterizing the reservoirs of the study area using 3-D seismic attributes. Hydrocarbon exploration of complex subsurface configuration as found in the study area requires an enhanced seismic interpretation approach. Several extracted seismic attributes which include variance, acoustic impedance, average energy, spectral decomposition, etc were used to enhance the interpretation of subtle hydrocarbon traps. Suites of signatures from wire-line logs and seismic volume were utilized to gain insight into the hydrocarbon saturated areas and the possible hosting (trapping) units outside the vicinity of well control. Well-to-seismic tie revealed that reservoir tops are tied to direct hydrocarbon indicators (Bright spots) on the vertical seismic section. Seismic variance attribute greatly enhanced geologic discontinuities and aided fault interpretation across the study area while spectral decomposition technique helped to delineate channel geometry and to appropriately select the best band for channel in-fill identification. Two major growth faults (F1 and F2, trending northwest to southeast respectively) were mapped at the central part of the field were revealed to have demarcated the field into three major blocks. Fault 1 (F1) has a southerly dip, while Fault 2 (F2) has a northerly dip. Six faults designated F1, F2, F4, F5, F6& F8 and four seismic horizons of interest were identified and mapped. Structural maps generated from the study revealed that the main hydrocarbon trapping mechanism in the field are fault closures. The trapping elements that can be distinguished include anticlinal dip closures, up thrown fault closures, and down thrown fault closures. Prospective hydrocarbon accumulation spots identified in the study area occur in the downthrown side of F1 and F2 and within the enclosed channel-fill sands in the “Bawi” Field. Four hydrocarbon bearing reservoirs (R1, R2, R3, and R4) were delineated. The reservoirs have an average porosity range of 19% to 38%; water saturation range of 28% to 44%, and net to gross range of 60% to 88%. Estimation of hydrocarbon volume in place revealed that R1 has less than a million cubic feet aof gas while R2 contains 795 million barrels of oil. Reservoirs R3 and R4 have estimated volume reserves of 177 and 227million barrels of oil respectively.

Keywords: Seismic attribute; spectral decomposition; reservoir characterization; petrophysics; reservoir; Niger delta.

1. Introduction

Innovative seismic attributes have the potential for revealing subtle geologic features from conventional seismic amplitude data. Chopra and Marfurt [1] defined seismic attribute as any measure of seismic data that helps the seismic interpreter to visually enhance or quantify features of interpretation interest. A seismic attribute is therefore any property of seismic data that helps us better visualize or quantify features of interpretation interest. Seismic attributes have proliferated in the last three decades at a rapid rate and have helped in making accurate predictions in hydrocarbon exploration and development [2]. They are most often widely used for lithological and petrophysical prediction of reservoir properties. Attributes are related to

the fundamental information in seismic data which include time, amplitude, frequency, and attenuation. Generally, time-derived attributes help to discern structural details while amplitude/frequency derived attributes are better suited for addressing problems of stratigraphy and reservoir characterization [44-45]. Amplitude attributes are the most robust and are most often used while frequency attributes may help to resolve problems associated with subtle stratigraphic traps and may reveal additional geologic layering [3]. One of the frequency attributes that has gained popularity and wide application in the hydrocarbon industry over the past few decades is spectral decomposition [46-47]. Spectral decomposition is an innovative seismic attribute used for reservoir imaging and interpretation technology [4]. The technology utilizes a sequence of seismic frequency slices through an area of interest to create a suite of frequency maps which can be selectively combined to yield much higher resolution images of reservoir boundaries, lithologic heterogeneities and interval thicknesses than traditional broad-band seismic displays [5]. Castagna *et al.* [6] mentioned four effects or ways in which spectral decomposition can help in the direct detection of hydrocarbons, which include: 1) abnormally high attenuation, 2) low-frequency shadows, 3) tuning frequency anomalies (also called differential reservoir reflectivity or preferential reservoir illumination), and 4) frequency-dependent Amplitude Variation with Offset (AVO).

Seismic attributes have evolved over the past three decades and have been invaluable in making far better accurate predictions and characterization of reservoir properties [7-11]. They are specifically applied in hydrocarbon exploration and development and are widely used for lithological and petrophysical prediction of reservoir properties [11]. Common seismic attributes such as complex trace [12], coherence [13], curvature [14], and spectral decomposition attributes [4] use mathematical formulations to capture the geometry or other physical properties of the subsurface and can be used to clarify subtle geologic features of interest [48-49]. A methodology has now been proposed and described for 3-D structural characterization based on the combination of specific attributes of interest and other visualization techniques [1,50-52]. The correct combination and sequence of these attributes can enhance the final goal of identifying features that were not visible before.

Radical development of new technology has led to the discovery of new attributes like texture attributes [15]. Sangree and Widmier's [15] pioneered this discovery which suggested that zones of common seismic signal character are related to the geologic environment in which their constituent sediments were deposited. This concept have been used by Love and Simaan [16] to attempt the extraction of patterns using texture analysis. Texture is defined by the spatial configuration of rock units and is more diagnostic of and relevant to deformational fabrics, depositional facies, and reservoir properties than an averaged acoustic property [17]. The methodology follows the way a seismic interpreter analyzes seismic amplitudes and waveforms. In the past decade, the idea of studying seismic 'textures' has been revived. While the term was earlier applied to seismic sections to pick out zones of common signal character [18], several studies have been carried out which use statistical methods to classify and clarify textural signatures using gray-level co-occurrence matrices [9-10,19-22]. Some of the statistical measures used are energy (denoting textural homogeneity), entropy (measuring predictability from one texel or voxel to another), contrast (emphasizing the difference in amplitude of neighboring voxels) and homogeneity (highlighting the overall smoothness of the amplitude). Homogeneity, contrast and entropy have been found to be the most effective in characterizing seismic data. Texture attributes are promising and can aid the geophysicist for making more accurate interpretations.

The evaluation of the intrinsic properties of a reservoir like thickness, net-to-gross ratio, pore fluid, porosity, permeability, water saturation and volumetric reserve is what is most often regarded as reservoir characterization [53-55]. Most of these reservoir properties were previously estimated using information from borehole logs. However, in the past few years, most of these properties have been mapped with the help of seismic attributes especially when calibrated with available well data within the study area [55-57]. This methodology has certain inherent advantages which includes the high spatial coverage as well as the fact that the

seismic data can be used for interpolating and extrapolating within and beyond the locations of the few available well data [23]. Seismic attributes are characteristics of a seismic data and often represented by analytical maps that aids the interpreter in better interpretation and visualization of geological features of interest [44,51,54]. This work would therefore focus among other things on showing how derived seismic attributes can be used to enhance seismic interpretation and reduce risks in prospect prediction. The ability of the seismic data to image the sub-surface and assess interpreted structures and their closures for potential reservoirs for hydrocarbon entrapment and accumulation will also be investigated.

2. Regional geology of the study area

The study area is located within the Greater Ughelli Depobelt of the Niger Delta basin, southern Nigeria as shown in Fig.1. The geology, stratigraphy, petroleum and structural geology of the Niger delta basin have been extensively discussed in several key publications [24-33]. The Niger Delta basin is a world class petroleum province which lies approximately within longitudes 4°E and 8°E and latitudes 4°N and 6°N [59-59]. Its areal extent is about 75,000km² with a clastic fill of about 12,000m [34]. It ranks amongst the world’s most prolific petroleum producing tertiary deltas that together account for about 5% of the world’s oil and gas reserves [60-61]. The onshore portion of the Niger Delta includes the geologic extent of the Tertiary Niger Delta (Akata-Agbada) Petroleum System and is delineated by the geology of southern Nigeria [35]. The northern boundary is the Benin flank - an east-northeast trending hinge line south of the West Africa basement massif [58-59]. The northeastern boundary is defined by outcrops of the Cretaceous on the Abakiliki High and further east (south-east) by the Calabar flank-a hinge line bordering the adjacent Precambrian rocks (Fig.2).

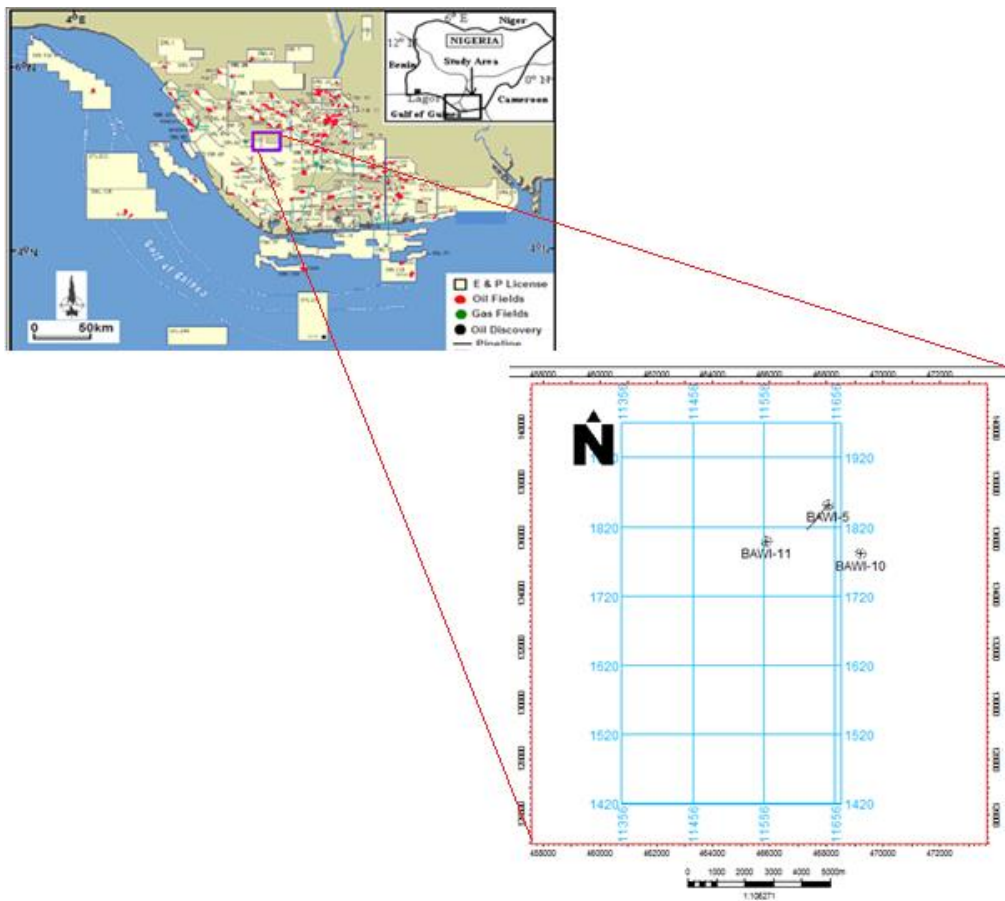


Fig.1a Base map and location of the study area showing the seismic lines and wells drilled

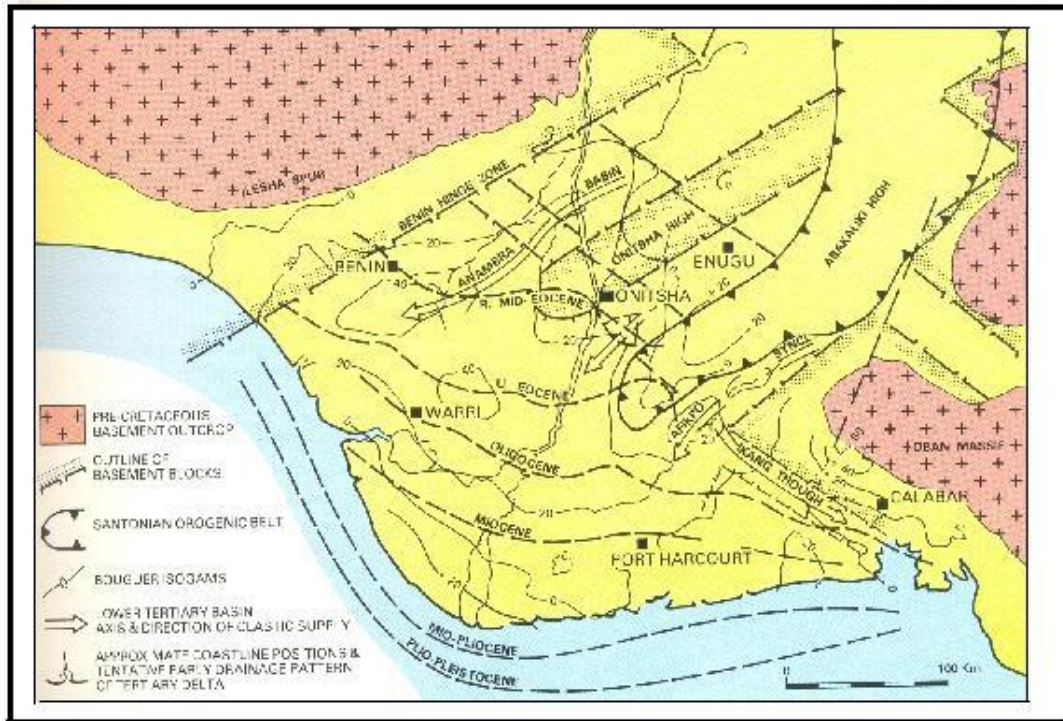


Fig. 1b. Geological map of the Niger Delta (modified after Whiteman [30])

The composite Tertiary sequence of the Niger Delta consists, in ascending order the Akata, Agbada and Benin Formation. The Akata Formation which is at the base of the delta is predominantly undercompacted, overpressured sequence of thick marine shales, clays and siltstones (potential source rock) with turbidite sandstones (potential reservoirs in deep water). It is estimated that the formation is up to 7,000 meters thick [28,36]. The Agbada Formation which is the major petroleum-bearing unit is about 3700m thick and is made up of an alternating sequence of paralic sandstones, clays and siltstone [24,35,37]. The upper Benin Formation overlying the Agbada Formation consists of massive, unconsolidated continental sandstones. These three major lithostratigraphic units decrease in age basin ward, reflecting the overall regression of depositional environments within the Niger Delta clastic wedge. The deposition of the three formations and the progradation of the Niger Delta has been dependent on the interaction between rates of subsidence and sediment supply, and modified by faulting. Several growth-fault bounded sedimentary units (depobelts) are therefore present. These depobelts succeeded one another as the delta prograded through time under the influence of off lapping siliciclastic sedimentation cycles [35,38]. Sedimentation in the depobelts is a function of sediment supply and of accommodation space created by basement subsidence and growth faulting. Growth faults, triggered by a pene-contemporaneous deformation of deltaic sediments are the dominant structural features in the Niger delta [60-61]. For any given depobelt, gravity tectonics were completed before deposition of the Benin Formation and are expressed in complex structures, including shale diapirs, rollover anticlines, collapsed growth fault crests, back-to-back features, and steeply dipping, closely spaced flank faults [24,39]. These faults mostly offset different parts of the Agbada Formation and flatten into detachment planes.

Petroleum in the Niger Delta is produced from sandstone and unconsolidated sands predominantly reservoir rocks of Eocene to Pliocene in age and are often stacked, ranging in thickness from less than 15 meters to about 45 meters [24]. Based on reservoir geometry and quality, the lateral variation in reservoir thickness is strongly controlled by growth faults, with the reservoir thickening towards the faults of the downthrown block [39].

3. Methodology

This research attempts to identify and characterize prospects in the "Bawi" field, Niger Delta through an integrated seismic attribute assisted interpretation of the study area. The well data used include well header, check shots, well deviation and well log data. Biostratigraphic information was only available for one well. Interpretative geophysical softwares utilized include Petrel 2013 and OpendTect 4.2.0. A quick look interpretation was carried out using gamma ray and resistivity logs for lithofacies and hydrocarbon pay zone (reservoir) determination of three wells (Bawi-11, Bawi-5& Bawi-10). Gamma ray log was used to delineate lithology (sand and shale bodies). Sand bodies were identified by deflection to the left due to the low concentration of radioactive minerals in sand while deflection to the right signifies shale which is as a result of high concentration of radioactive minerals. Reservoirs were identified by using the log signatures of both gamma and deep resistivity logs. Intervals that have high resistivity are considered to be hydrocarbons while low resistivity zones are thought to be water bearing.

Well correlation was carried out to determine the continuity and equivalence of lithologic units for the reservoir sands and marker sealing shales of the wells in the study area (Figs.2&3). Regional markers from biostratigraphic information obtained for well 3(Bawi-10), were matched on the Niger Delta chronostratigraphic chart for maximum flooding surfaces determination and correlated across the field using the gamma ray log motifs. The gamma ray log motif was used for an initial lithologic interpretation to identify the major sandstone and shale units, and then further combined with the deep resistivity logs for detailed correlation work with emphasis on the shale sections. Four reservoirs of interest R1, R2, R3&R4 were identified and correlated in the Oil field. Reservoir tops sand 001, sand 002, sand 003 and sand 004 were correlated to depths of 2886 m, 3527m, 3856m and 4024m in Bawi-11 and 3160m, 3850m, 4000m and 4177m in Bawi-5. Well section analysis revealed that each of the sand units were revealed to extend through the field and vary from 70 to 77m in R1, 63 to 73m in R2, 45 to 64m in R3 and 35 to 50m in R4. Some sand units occur at greater depth than their adjacent units (possibly an evidence of faulting). The shale layers were observed to increase with depth along with a corresponding decrease in sand layers.

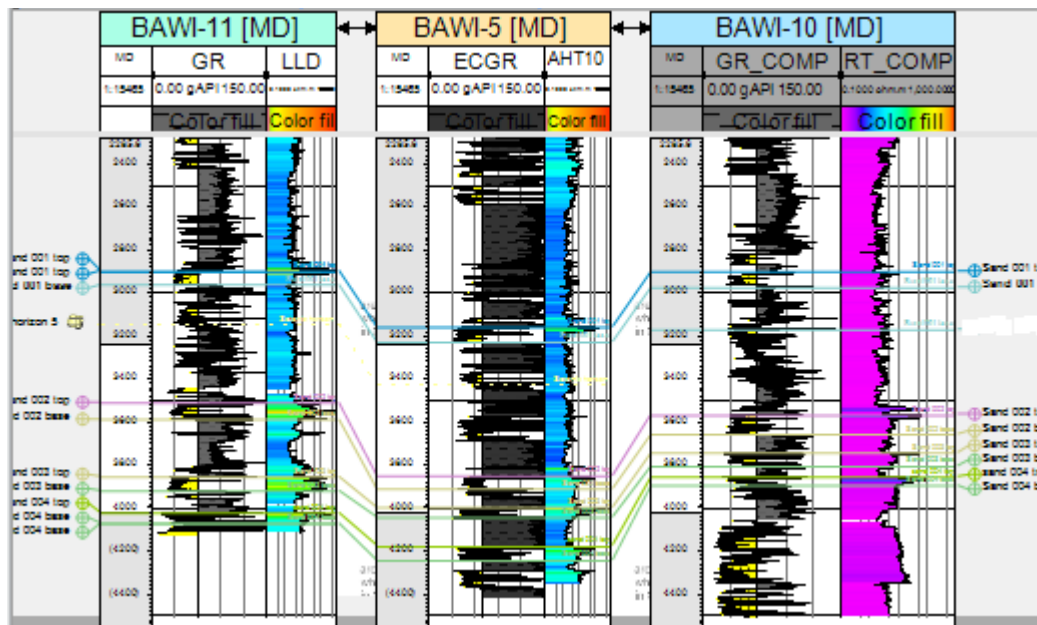


Figure 2. Display of Well log correlation across the Oil field

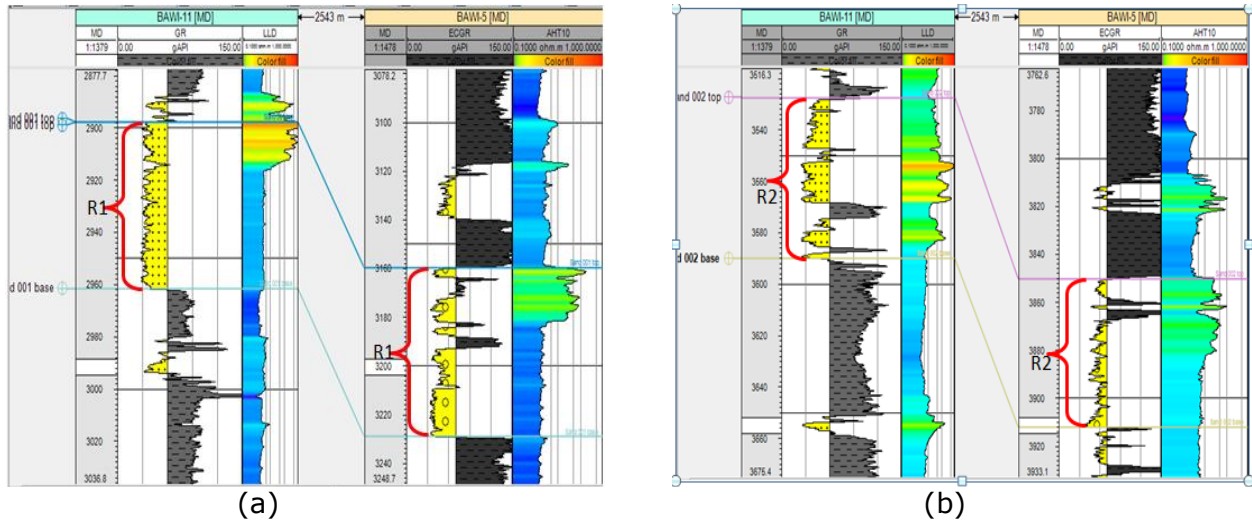


Figure 3a. Reservoir delineation from well logs (a) Reservoir R1 (b) Reservoir R2

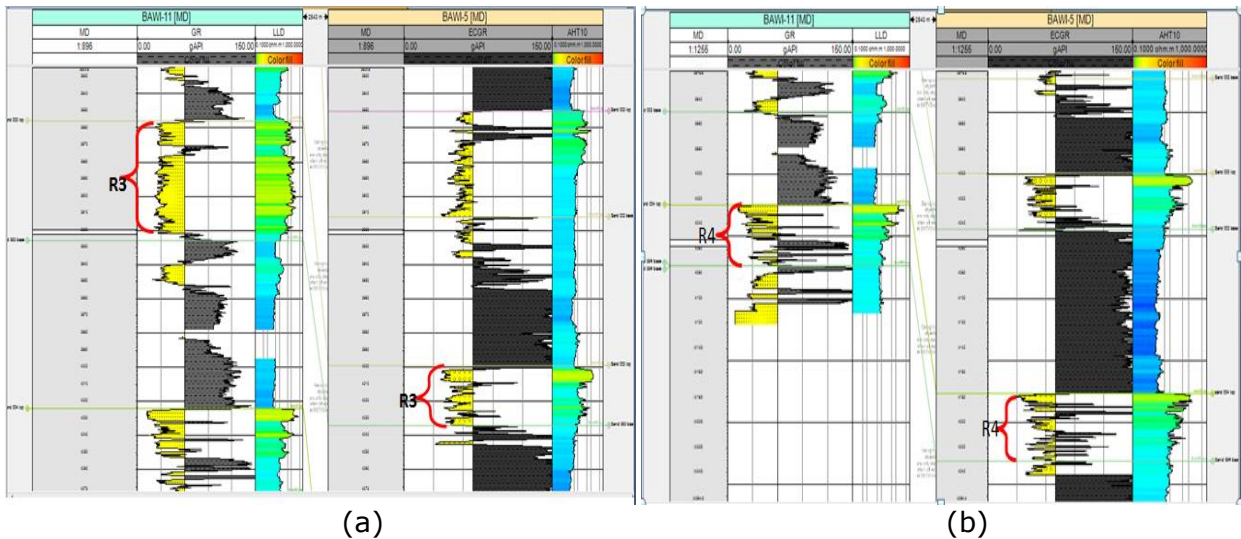


Figure 3b. Reservoir delineation from well logs (a) Reservoir R3 (b) Reservoir R4

Similarly, well to seismic tie was carried out with information extracted from Bawi- 11 well, in order to calibrate the seismic data and also identify its polarity (Fig.4).A synthetic seismogram was generated for this purpose, using sonic and density logs. First, corrected sonic and density logs was used to generate the Acoustic impedance and a reflection coefficient was computed. The generated reflection coefficient was convolved with extracted wavelet from the seismic (zero phase wavelet) to generate the synthetic seismogram. Well to seismic correlation revealed that reservoir tops tied to bright reflections on seismic sections. High amplitudes were interpreted as peaks, while low amplitudes represent troughs.

4. Result interpretation and discussion

4.1. Horizon picking, fault Mapping and map generation

The seismic reflection data quality was low in certain places and therefore fault trends were not readily apparent on seismic sections due to poor resolution. Seismic variance attribute was employed to reveal subtle details in the seismic data and to guide fault mapping. Major and minor faults were mapped based on linear features observed in the seismic data. Key reflections corresponding to well tops on seismic sections were identified and mapped across

the seismic volume. Four horizons were picked in both in lines and cross lines. Interpretations were first made in the volume near the wells that were tied, and then extended outwards from the well. Seismic attribute (Relative acoustic impedance) showed great promise for determining reflector continuity. Time maps were generated from the picked horizons, and fault polygons developed. Furthermore, a velocity function generated from the T-Z data was used to convert the time maps to depth maps.

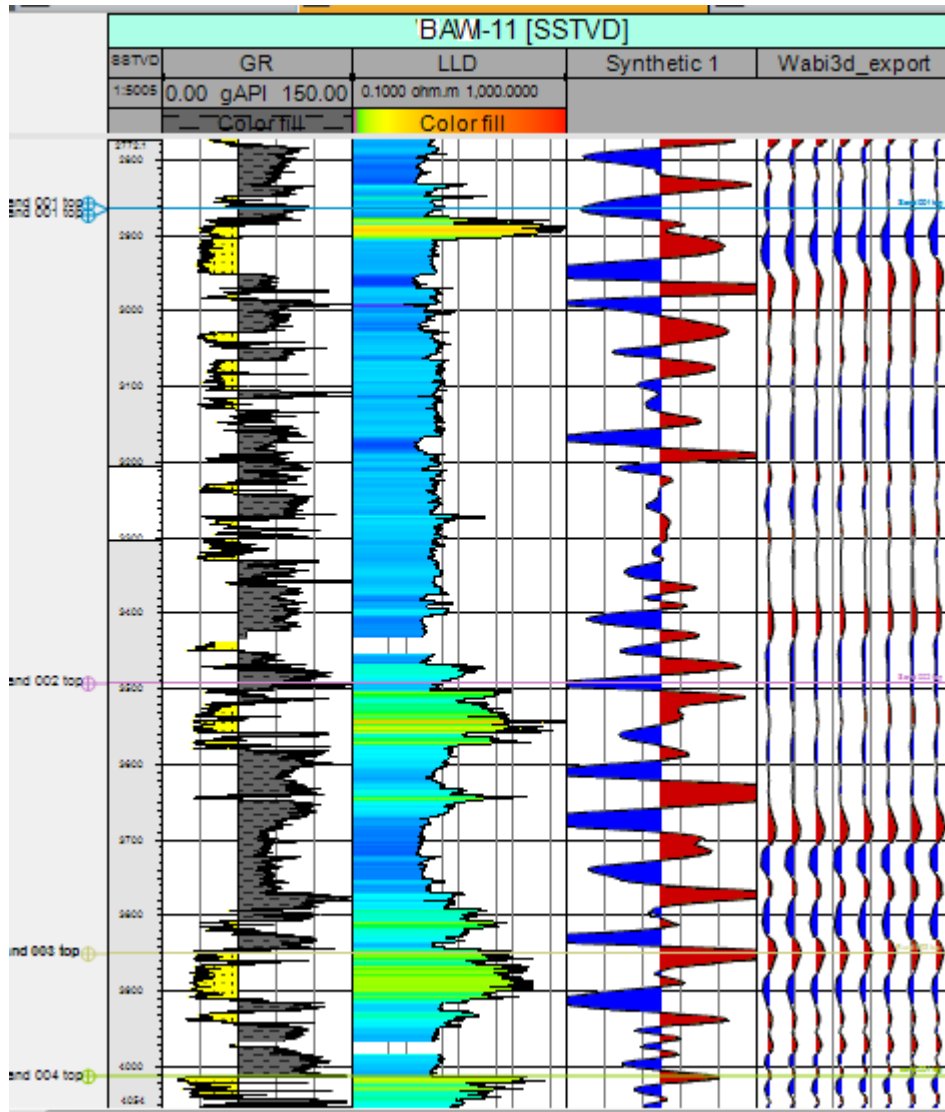


Figure 4. Well to Seismic tie section (Bawi-11). High amplitude events correspond to peaks

Seismic variance attribute revealed discontinuities on seismic sections and aided fault interpretation. Structural interpretation of the study area revealed a preponderance of northwest to southeast (NW-SE) trending faults in the field (Fig. 5). Two major growth faults (F1 and F2) were mapped at the central part of the field thereby dividing the field into three major blocks. These faults are the major structure building faults. These two faults extend throughout the field as seen on the interpreted seismic sections. Fault (F1) is dipping to the south while fault (F2) is dipping to the north. Other faults mapped include a synthetic fault (F5), and minor faults (F4, F6 and F8). Displacement of seismic facies across the faults generally increased with depth. This could be attributed to sediment deposition on the downthrown part of the fault.

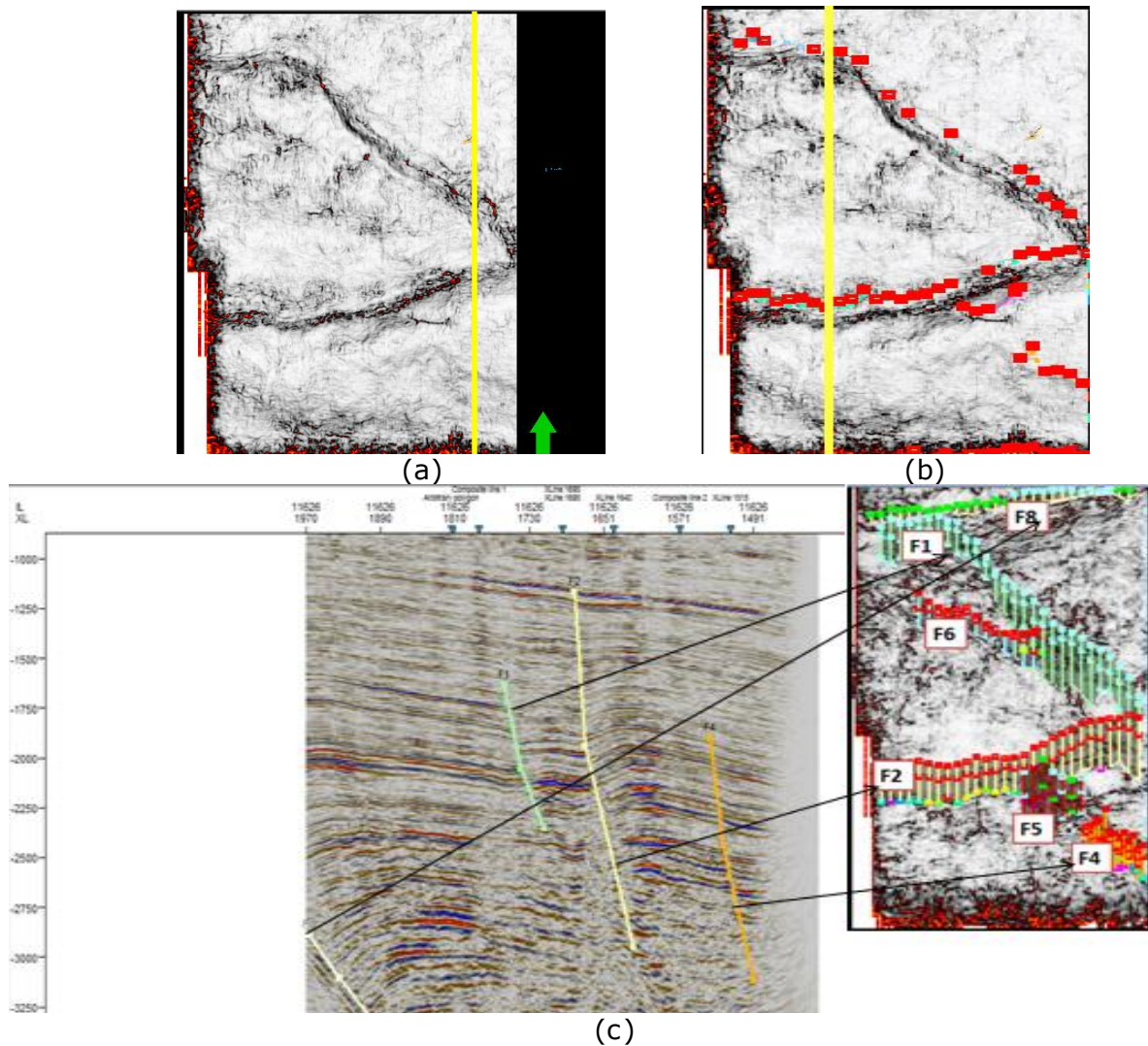


Figure 5. (a) Variance slice at 2000ms (b) Variance slice at 2000ms with fault sticks of picked faults (c) Faults picked on seismic section (inline 11626) and corresponding fault sticks on variance slice (2900ms)

Key seismic reflections identified were moderately continuous and truncated in places by faults. Altogether, four horizons were picked on both in lines and cross lines across the field (fig. 6). Time structure maps were generated from the picked horizons with depth structure maps depth converted from the time maps using a velocity model (Figs.7- 10). The depth converted map of the horizons reflected the structure of the subsurface. Large faulted anticline take up most of the study area. The anticline trends NE- SW and is asymmetrical in shape. The complexity of the anticline increases from the top (horizon 1) to the bottom (horizon 4). This field is characteristically associated with fault closures and roll-over anticlines, which are considered to be the main hydrocarbon trapping mechanisms.

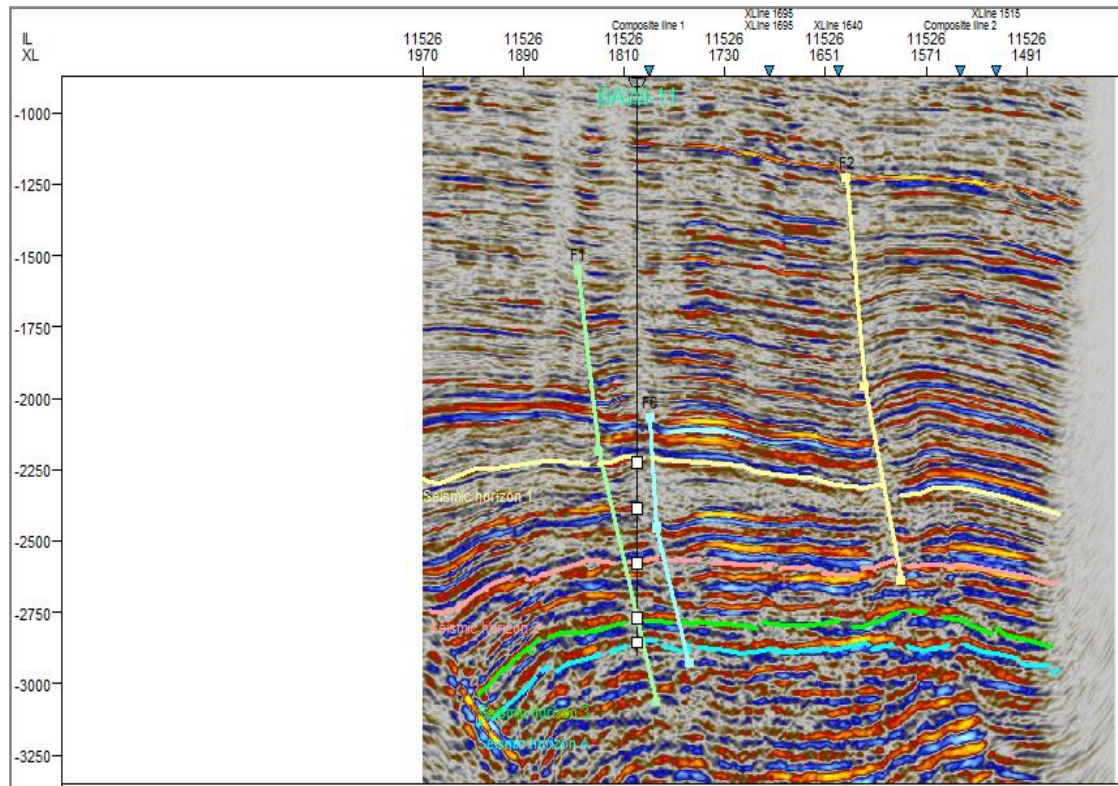


Figure 6. Showing Acoustic impedance attribute enhanced reflections and picked horizons (inline 11526)

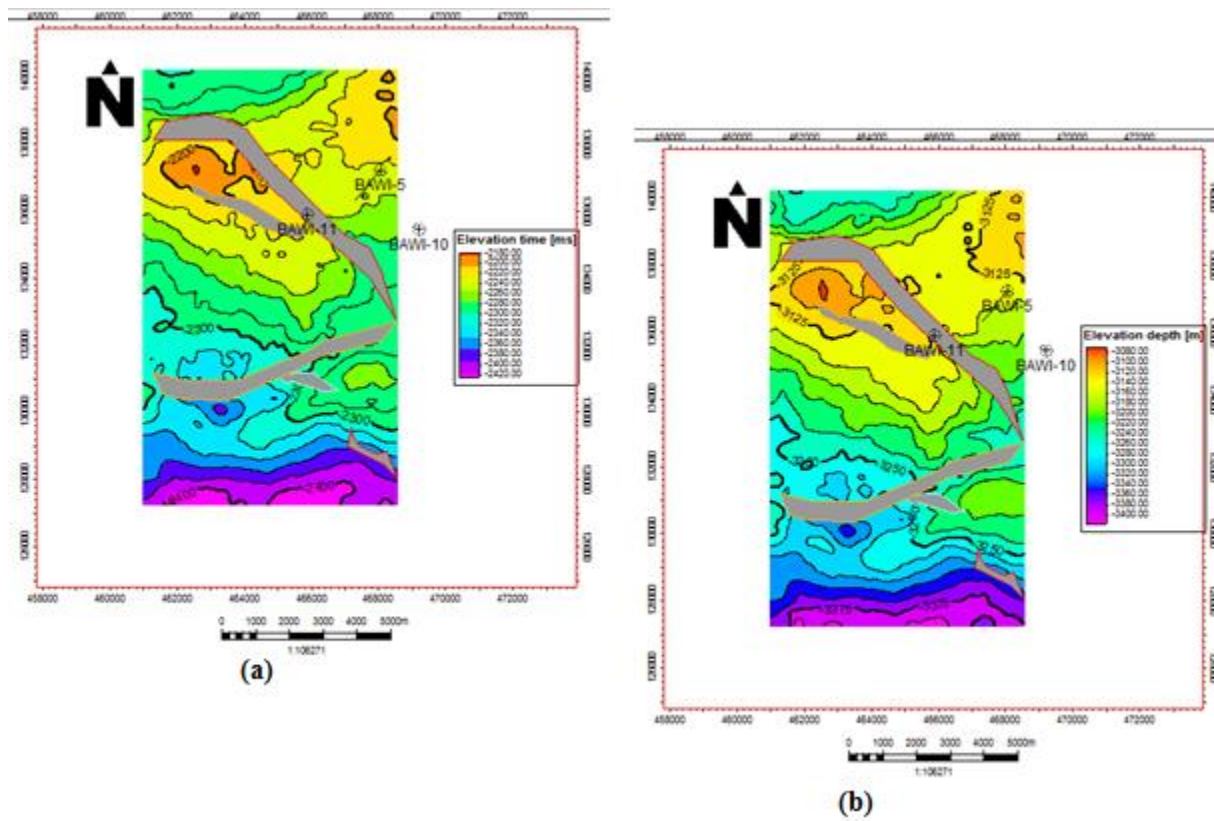


Figure 7. Structural maps from horizon 1 (a) Time map (b) Depth map

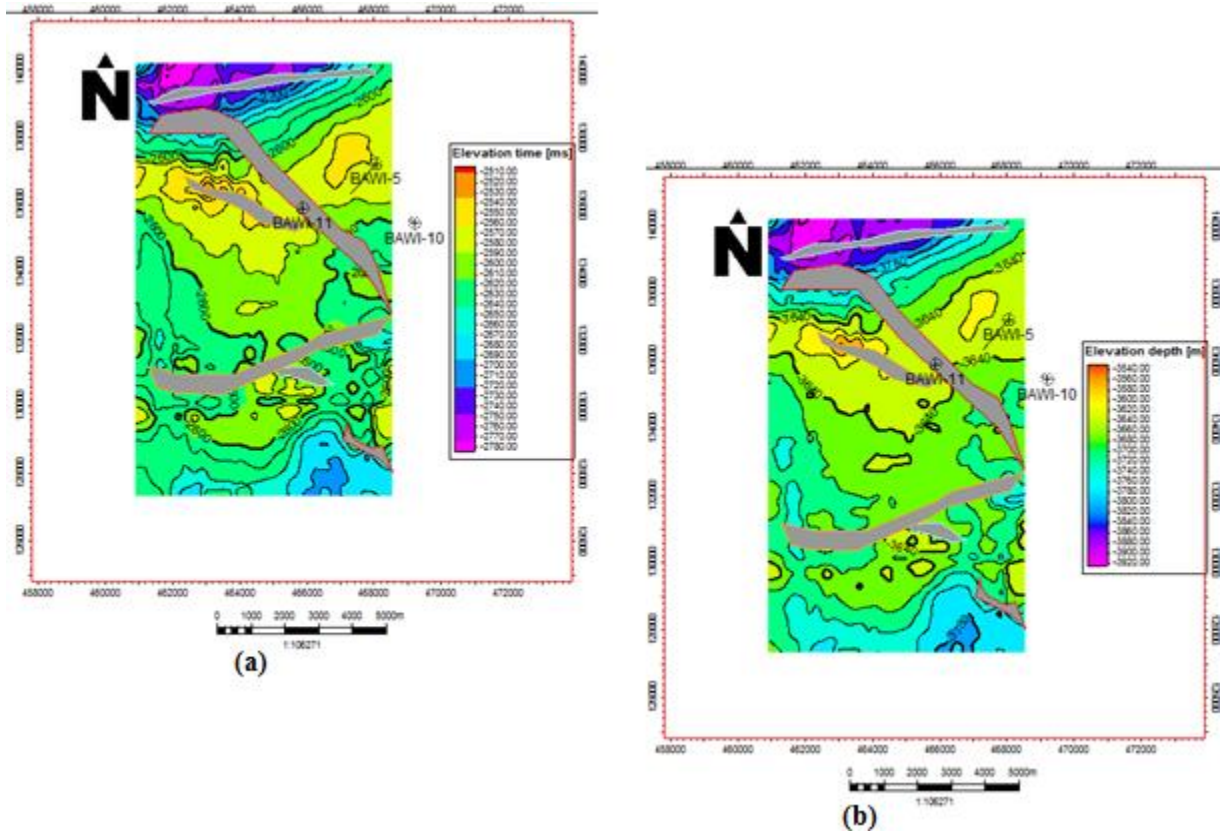


Figure 8. Structural maps from horizon 2: (a) Time map (b) Depth map

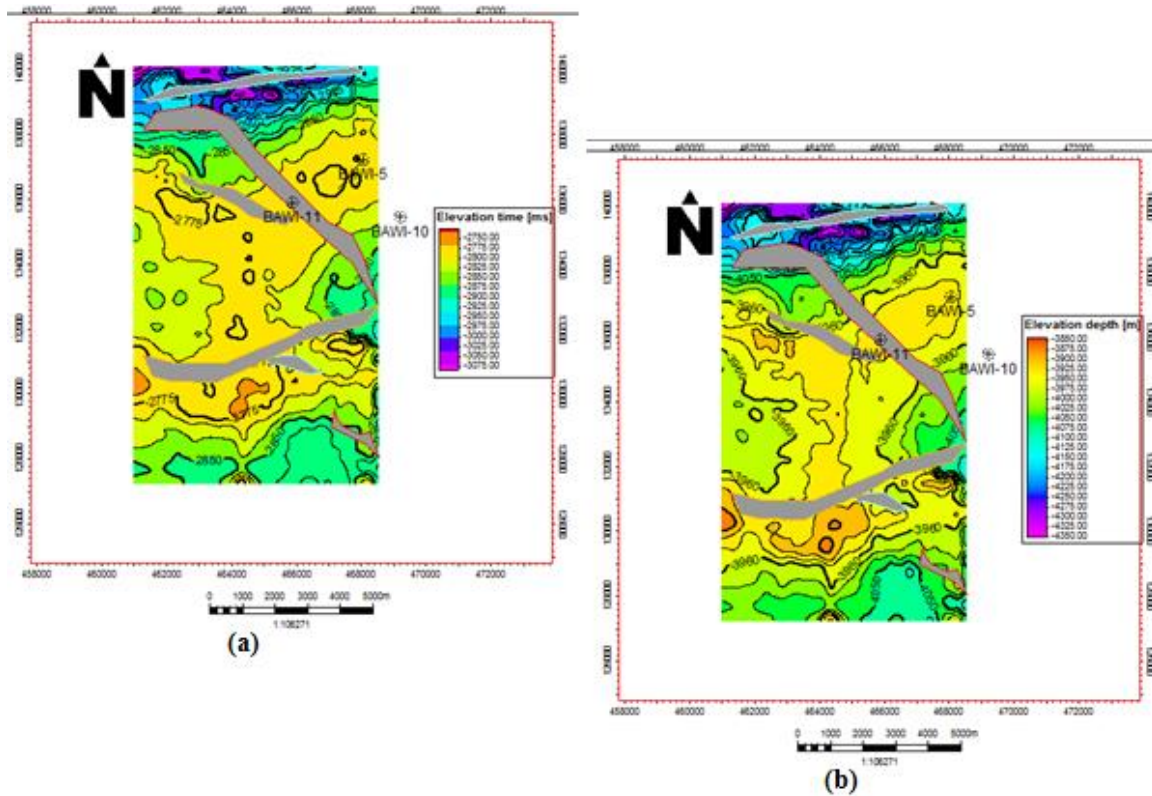


Figure 9. Structural maps from horizon 3: (a) Time map (b) Depth map

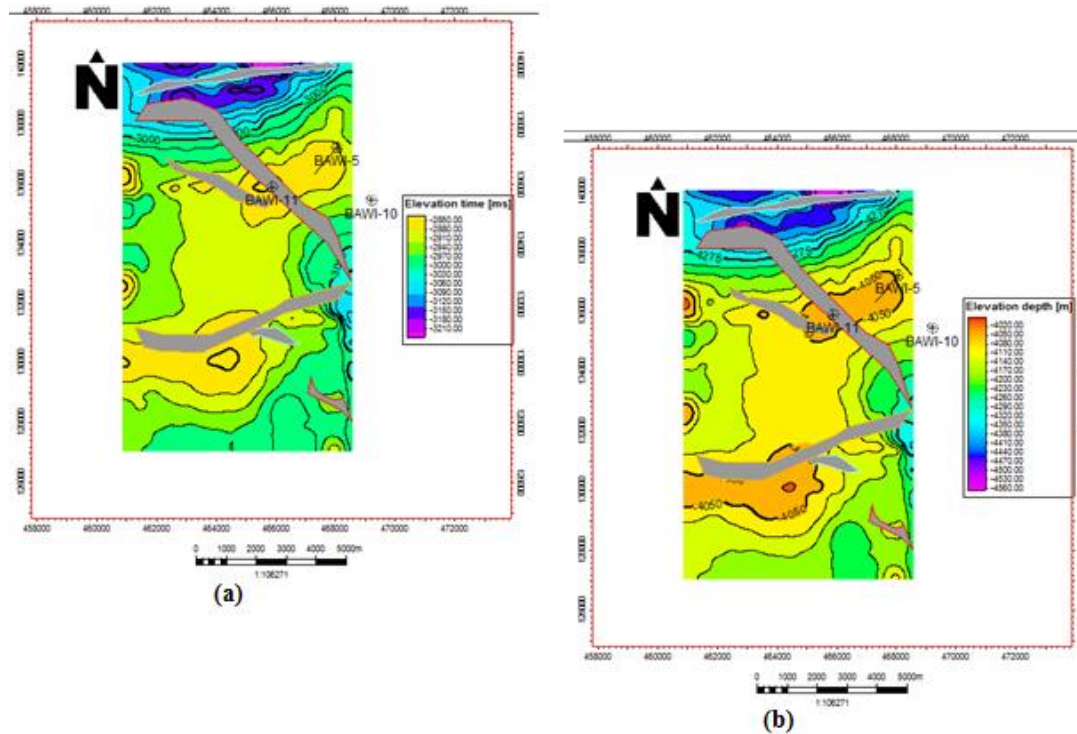


Figure 10. Structural maps from horizon 4: (a) Time map (b) Depth map

4.2. Seismic attribute analysis

The acronym DHI refers to Direct Hydrocarbon Indicators. DHI attributes are attributes that when observed in a seismic horizon, they indicate directly the presence of hydrocarbon to a very high degree. The primary DHI attribute used for this work was the average energy, which predicts areas of high amplitudes. The average energy was complemented by other seismic attributes which include instantaneous bandwidth attribute (to detect relative uniformity or otherwise of predicted lithology), and relative acoustic impedance attribute (a porosity indicator). Similarly, stratigraphic channel investigation was carried out in the study area using a combination of envelope, iso-frequency, and spectral decomposition. Spectral decomposition helped to generate series of maps in order to observe the response of reservoir characteristics to different frequency bands. These were integrated to determine the part of the channel with thickest reservoir continuity.

From the average energy map, higher energy spots are believed to be indicative of hydrocarbon (Fig. 11a). Variation in the Instantaneous bandwidth suggests sharper amplitude changes related to changes in lithology, while zero instantaneous bandwidth represents uniform lithology (Figs. 11b&11c). Although the exact lithology type may not be predictable, it gives an idea about where the lithofacies are uniform in the reservoir. The Relative Acoustic Impedance (RAI) is a porosity indicator. There is a high negative correlation between porosity and acoustic impedance. Bouvier *et al.* [36] reported that acoustic impedance contrast is negative for hard shale to soft sandstone and that in Nigeria, sandstones have comparatively lower acoustic impedance than shales; hydrocarbon bearing sandstones having even lower acoustic impedance than water-bearing sandstones with increased positive amplitude. By comparing with generated Relative Acoustic Impedance map, the lithology types associated with areas with uniform lithology (zero bandwidth) are assumed to be sands (because of associated high porosity). This is confirmed by good match between gamma ray and instantaneous bandwidth at well locations. This guided our prospect prediction. Identified prospects are labeled P1, P2 and P3 (Figs. 11-13).

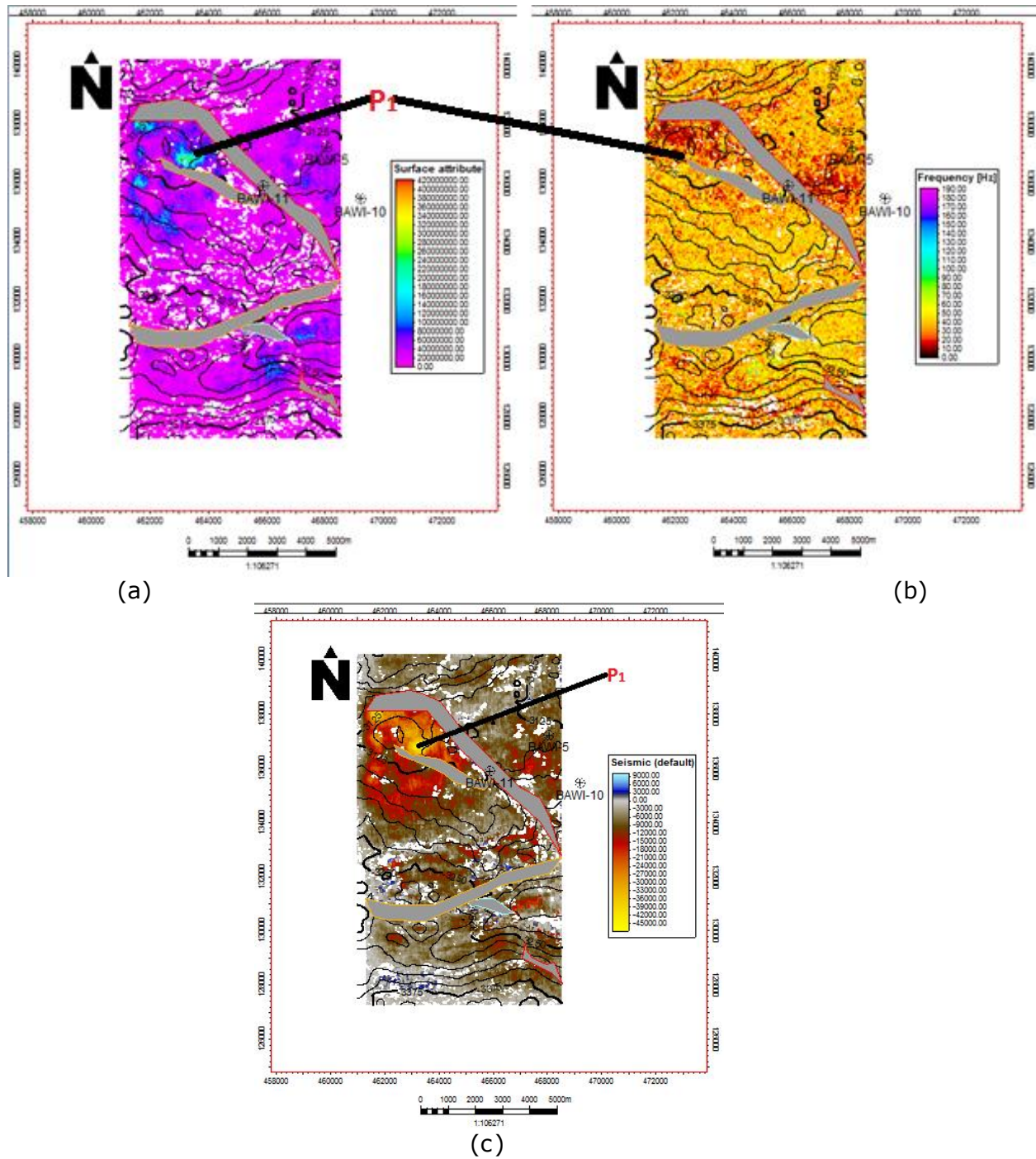


Figure 11. Seismic attribute analysis for horizon 1. Prospective area P1 was identified (a) Average energy (b) Instantaneous bandwidth (c) Relative acoustic impedance

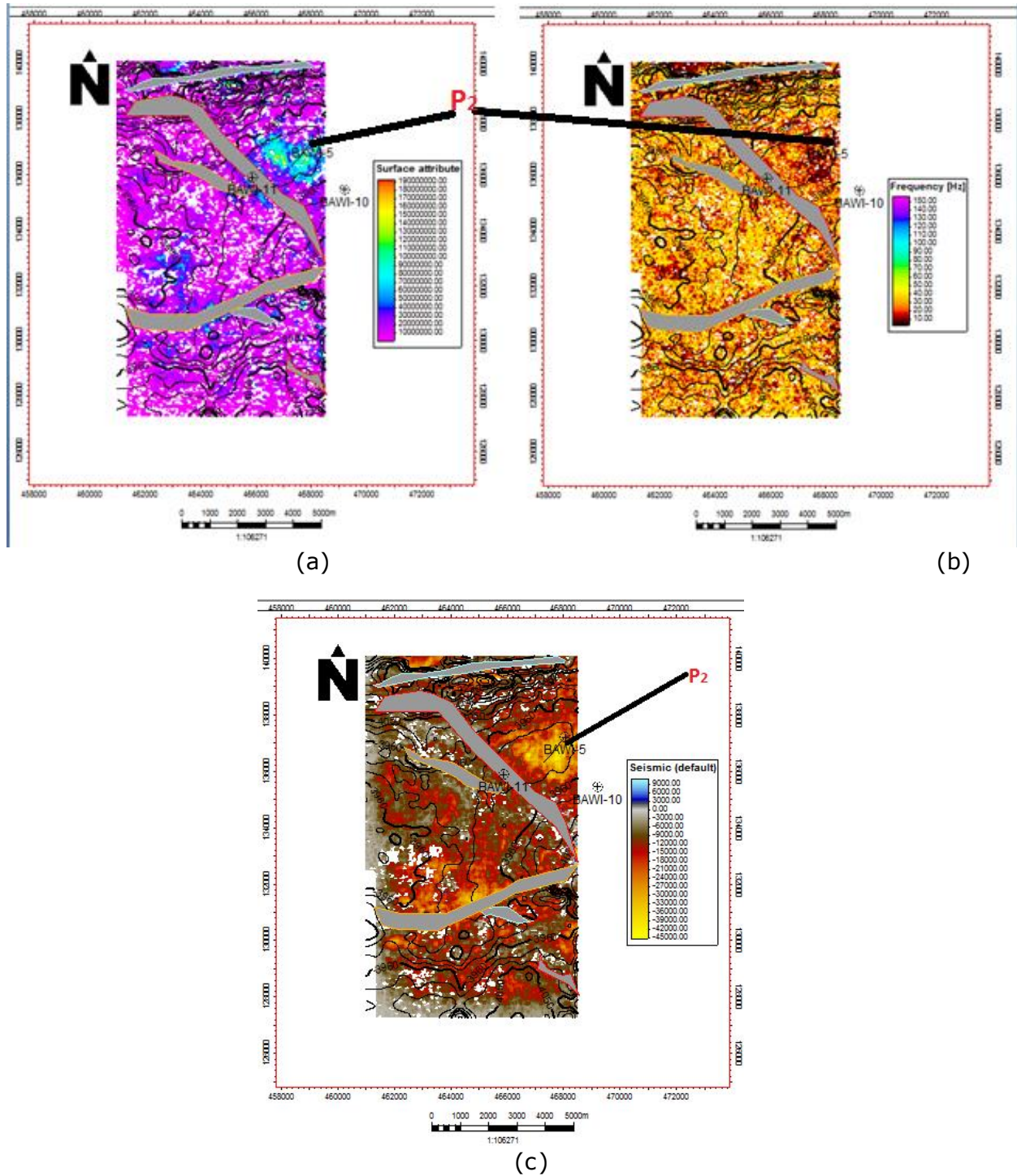


Figure 12. Seismic attribute analysis for horizon 3. Prospective area P2 was identified (a) Average energy (b) Instantaneous bandwidth (c) Relative acoustic impedance

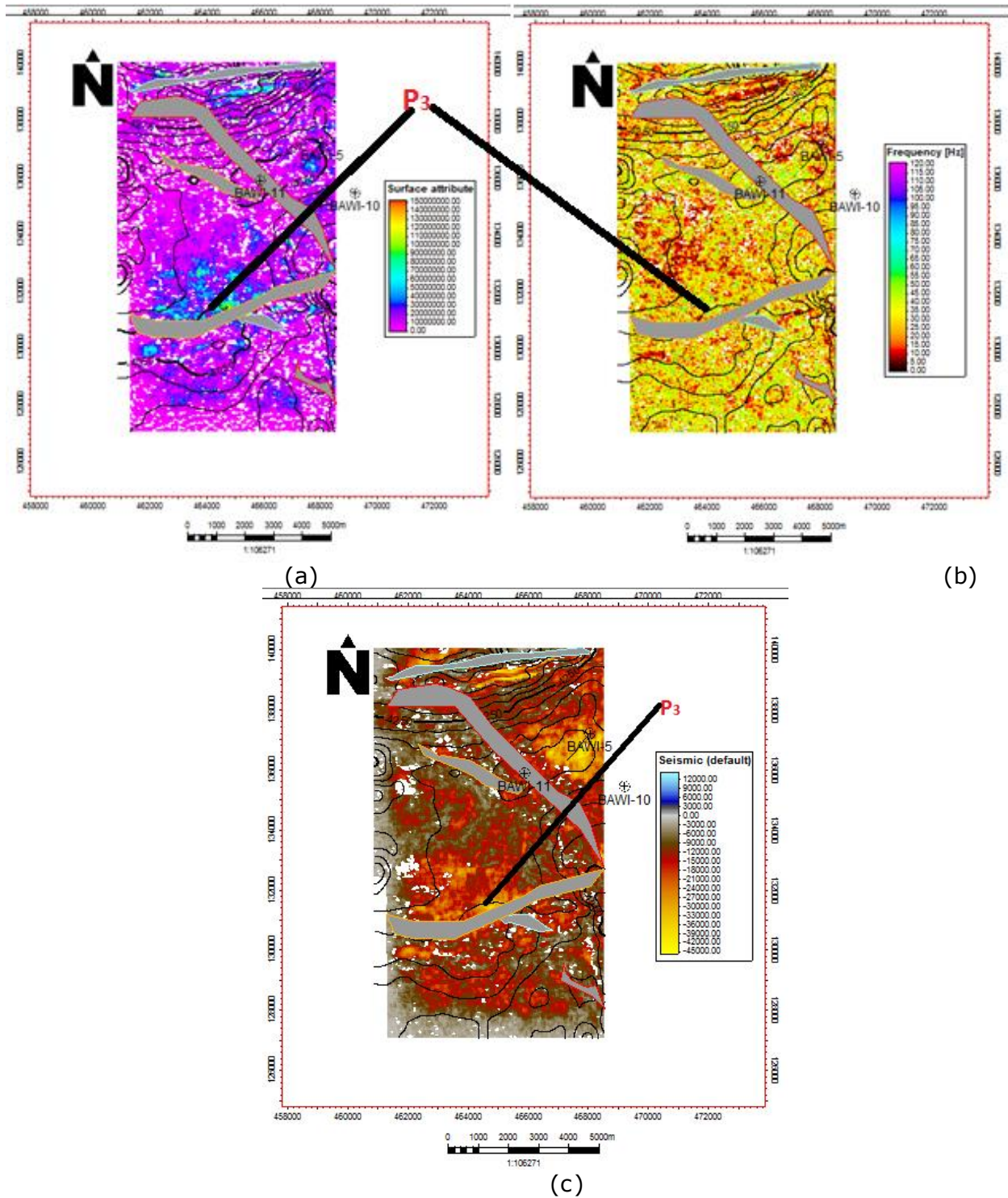


Figure 13. Seismic attribute analysis for horizon 1. Prospective area P3 was identified (a) Average energy (b) Instantaneous bandwidth (c) Relative acoustic impedance

4.3. Stratigraphic channel investigation

Sinuuous features were conspicuous at time slice 2600ms in the default seismic section. The observed features were further analyzed using seismic attributes. The time-slice (default seismic) and derived seismic attribute slices (Iso-frequency component and Envelop) are as shown in figure 14 below.

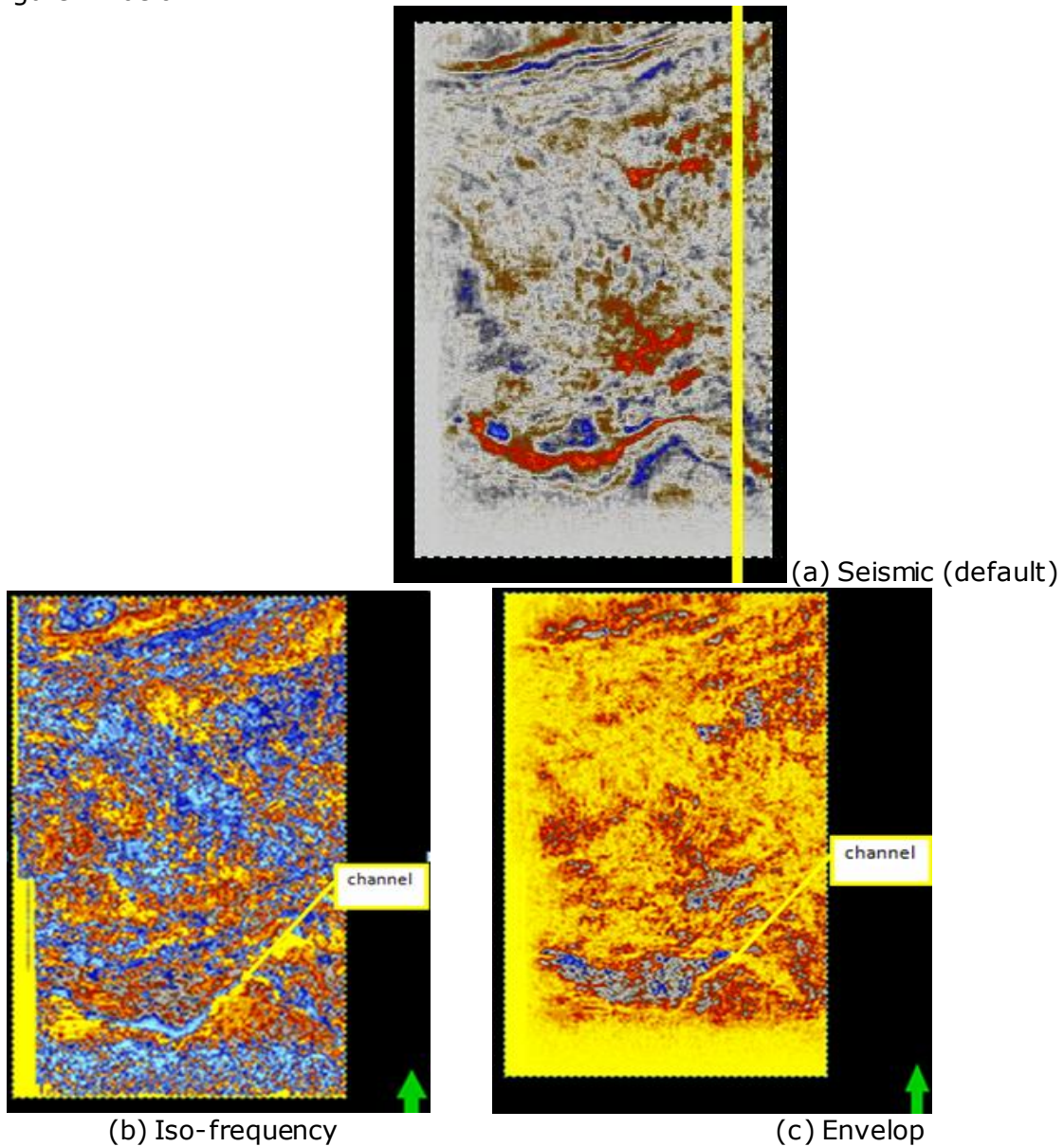


Figure 14. Time slice and derived seismic attribute slices at 2600ms (a) Seismic (default) (b) Iso-frequency (c) Envelop

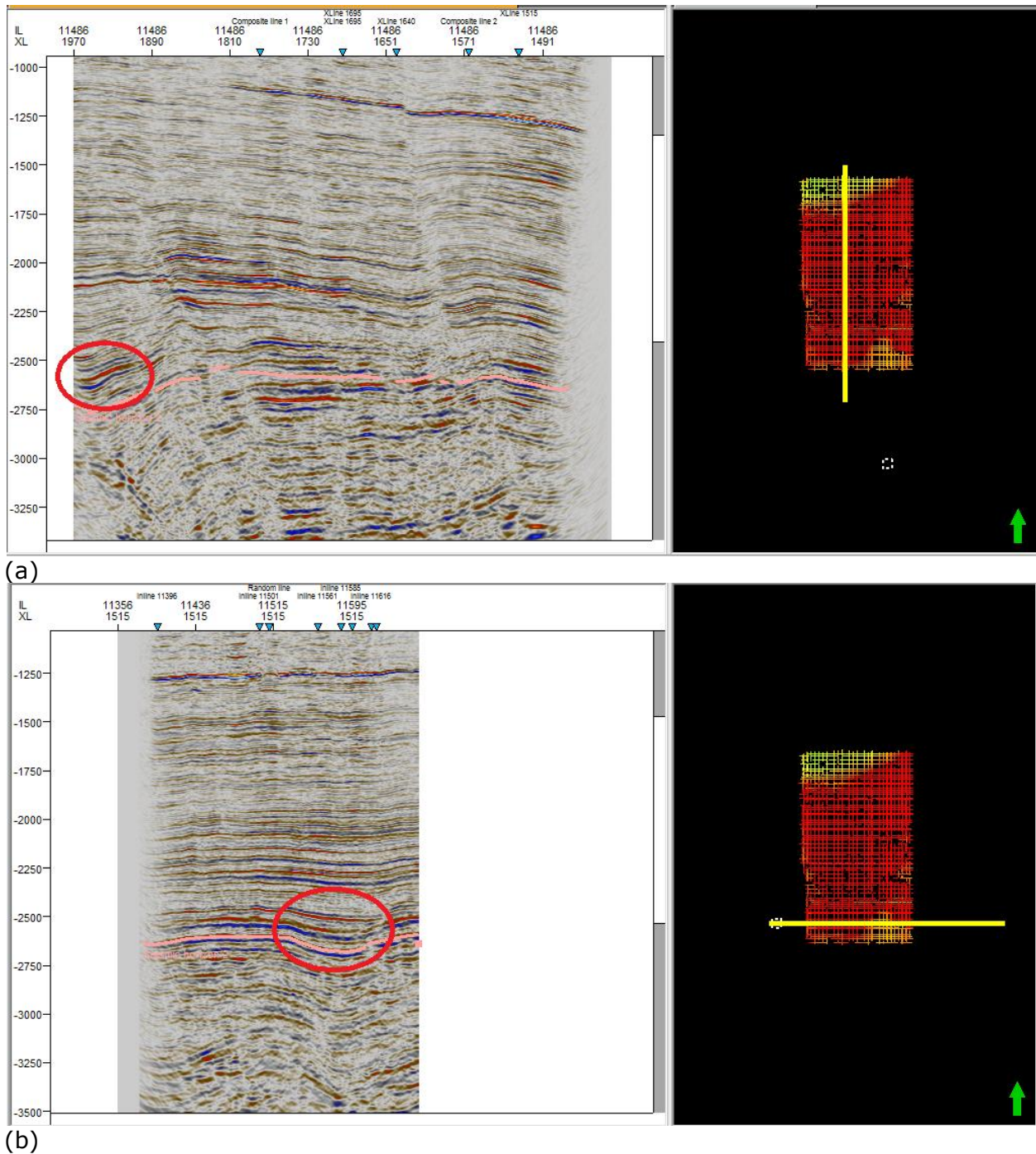


Figure 15. (a) Channel observed around 2600ms on seismic section (Inline 11486) (b) Channel observed around 2600ms on seismic section (Inline 1515). For both the inline and crossline - horizon picked (horizon 2) passed through channel region.

The sinuous features seen were confirmed to be channels from the seismic sections of inline 11486 and cross line 11436 are shown in figure 15 above. However, it was observed that the channel geometry shown by Iso-frequency attribute as seen on generated attribute map differs substantially from that on the generated envelop attribute map (Fig. 14). This observation suggests that we could be dealing with stacked and amalgamated channels. To resolve some of the subtle characteristics of the channel, spectral decomposition was employed which better

improved channel imaging and thickness delineation. The concept behind spectral decomposition is that, a reflection from a thin bed has characteristic expression in the frequency domain that is indicative of temporal bed thickness. In other words, higher frequencies image thinner beds better, and lower frequencies image thicker beds. The spectral decomposition workflow focused on processing Discrete Fourier Transform (DFT) at time slice 2600ms, transforming the amplitude/phase data into the frequency domain. Prior to running the spectral decomposition, 3-D seismic data was loaded on the OpenD Tect software and the dominant frequency of the seismic data determined (approximately 35Hz) as shown in figure 16 below.

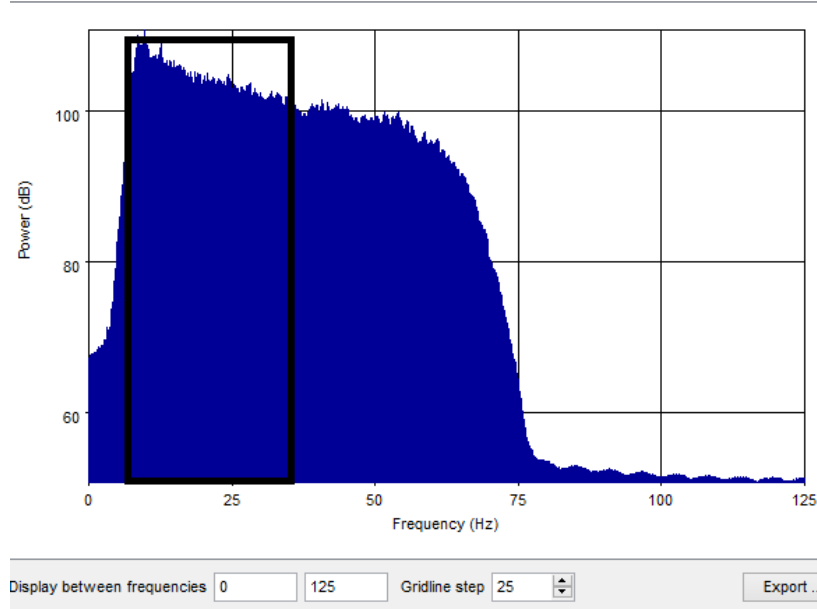


Figure 16. Amplitude spectrum for the Bawi Field. The dominant frequency band is highlighted.

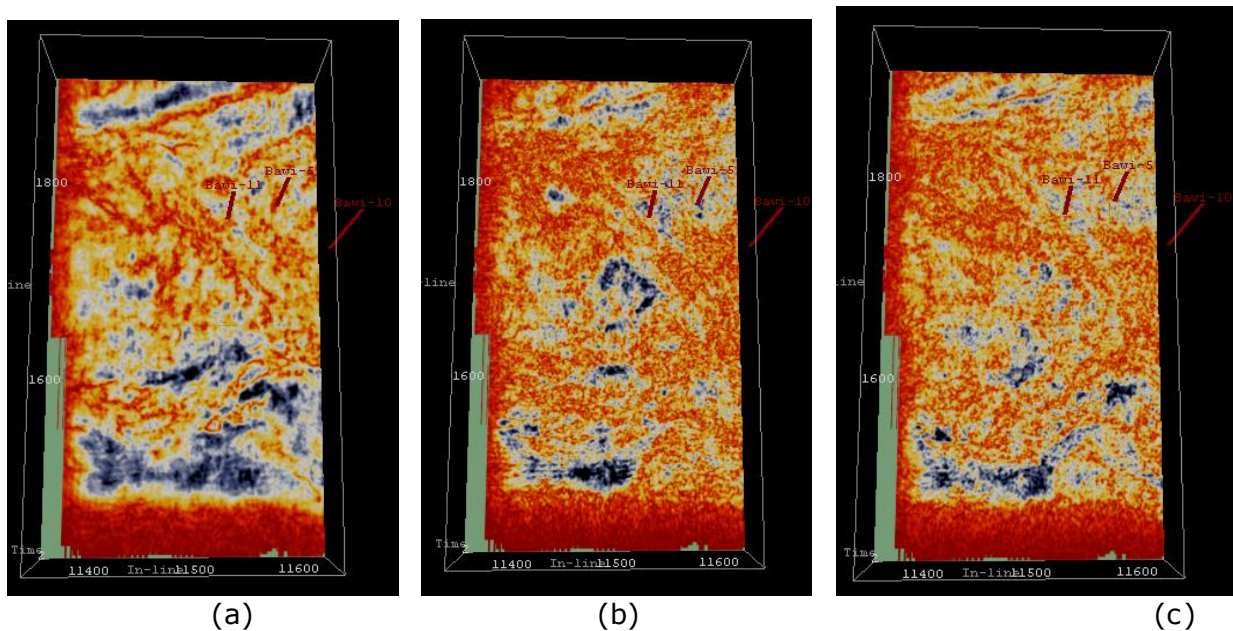


Figure 17. Spectral decomposition of seismic data at time slice 2600ms showing channel-fill sand (a) 5Hz (the lowest frequency band) (b) 35Hz (the dominant frequency band) (c) 70Hz (the highest frequency band).

Where we have a stratigraphic feature that varies in thickness, if the frequency content is high, thinner stratigraphic features will be “tuned in” and highlighted by higher amplitude. But, if the frequency content is lower, thicker stratigraphic features will stand out [41]. Typically, amplitude maps are dominated by the frequency content of seismic data and will best image stratigraphy with thickness related to the dominant frequency. The channel fill tuning frequency therefore may be either greater or less than the overall seismic dominant frequency (approximately 35Hz).

Based on the above theory, we incorporated the highest frequency band and lowest frequency band in our analysis as shown in figure 17. When we observed the response of the reservoir to different frequencies, it was discovered that 5Hz best imaged the channel feature in the lowest frequency band while 70Hz best imaged the channel in the highest frequency band. We used the Red-Green-Blue (RGB) colour blended map to integrate maps derived from our analysis. Each colour correspond to a specified frequency band i.e. 5Hz (lowest frequency band in Red colour), 35Hz (dominant frequency band in Green colour), and 70Hz (highest frequency band in Blue colour); see fig.17. The colors when additively combined produced the full-spectrum image shown in fig.17. White hue shows that the red (5Hz), green (35Hz) and blue (70Hz) have coincident high amplitude responses in that area (Fig.18). This is the part of the channel with the thickest reservoir.

Comparing the results of the spectral decomposition with the average energy attribute map of horizon 2, the thickest part of the channel can be seen to match a strong amplitude anomaly (Fig.19). Following the correlation observed on relative acoustic impedance attribute map, the lithology was interpreted as high porosity sand (Fig.19). This makes this part of the channel a good drilling location for hydrocarbon.

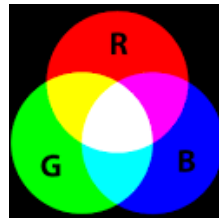
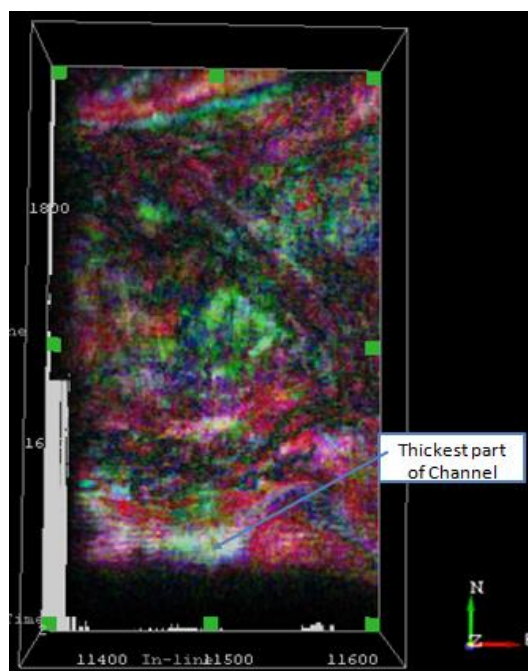


Figure 18. Colour blended frequency map showing the thickest part of the channel-fill sand. Note that the thickest part of the channel appear in white colour (all frequency ranges are present). The three colors used are shown in the color code.

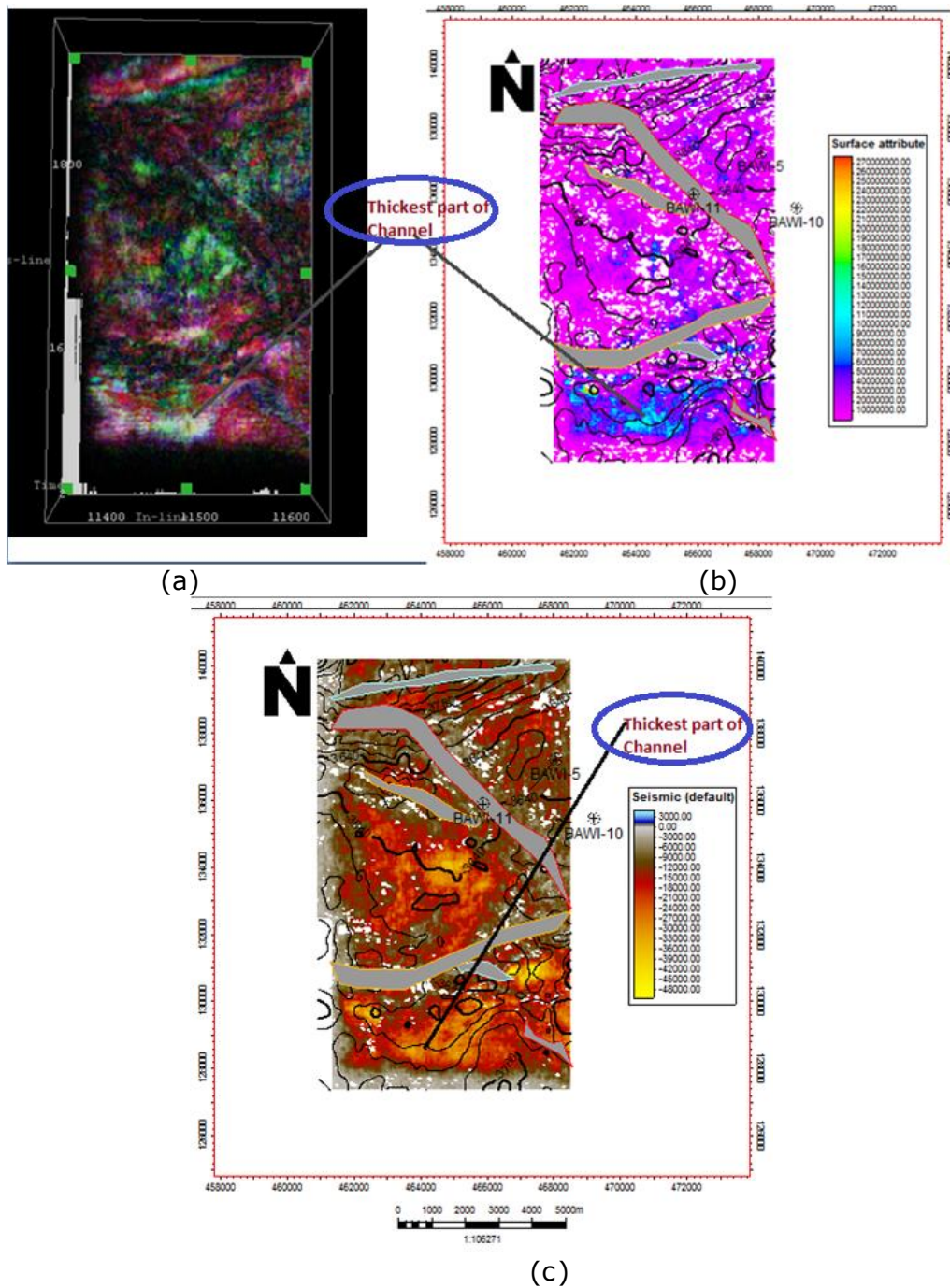


Figure 19. Seismic attribute analysis of channel-fill sand (a) Colour blended frequency map (b) Average energy attribute map of horizon 2 (c) Relative Acoustic Impedance map of horizon 2

4.4. 3-D Model generation of the study

Several models were then generated for the interpreted horizons to gain more information of interpretation interest. Models generated include 3-D structural models of the field, structural model based on seismic observation, and a general fault model of the field. The generated subsurface fault model of the study area is shown in fig.20. Fault models help to better appreciate fault relationships and assist in reservoir studies (Fig.20).The generated fault model revealed cross-fault juxtaposition around the central part of the study area. Cross-fault

juxtaposition is the most important fault seal process [40], as examples of capillary sealing by faulted rocks are fewer and more difficult to predict.

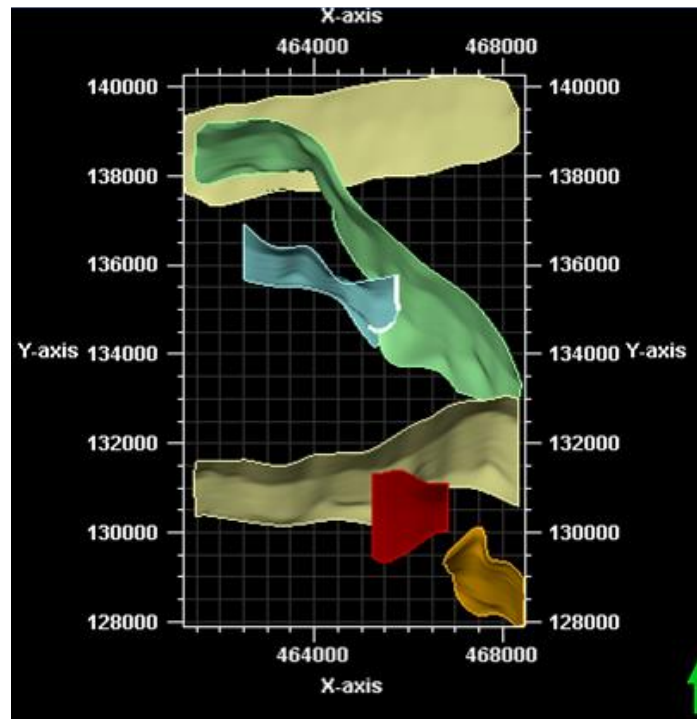


Figure 20. Showing a fault model of the field. Observe that one fault (F6) is cross-juxtaposed against another fault (F1) at the central part of the field. This has implications for the sealing capacity of the faults

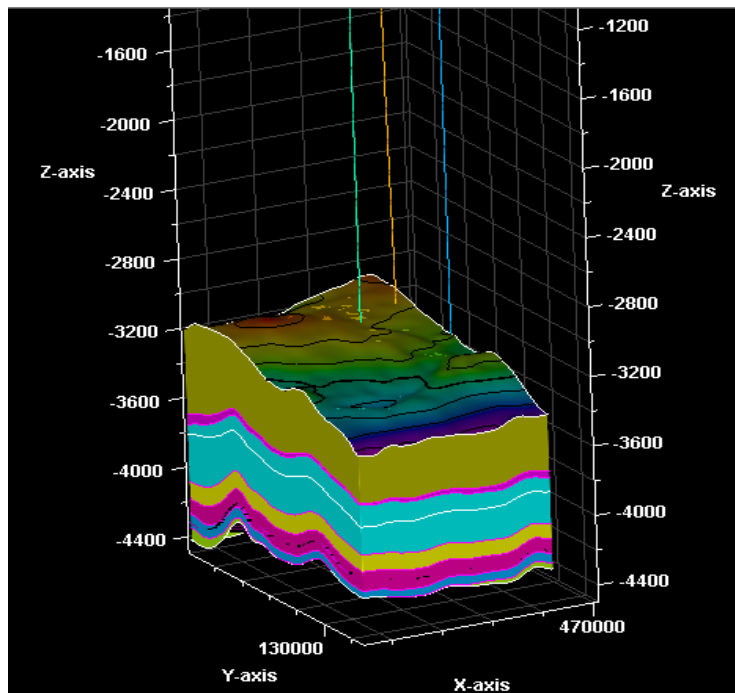


Figure 21. Showing 3D structural model of the Agbada sands (Bawi field). Compressional style deformation is observed. Displacements (upthrow/downthrow) caused by two major structure building faults in the field are better understood.

3-D structural models generated from the study area also revealed an anticline trending towards the southwestern part of the oil field. A smaller anticline trends to the southeastern part of the field. Structural highs are observed to be followed by a compression axis, and then structural lows. This could be a regressive trend towards the south of the Oil field. The models show clear evidence of compression style deformation (Fig. 21). Displacements (up throw/down throw) caused by the two major structure building faults in the field are therefore better understood from this model.

An amplitude supported structural model generated shows maximum amplitude attribute extracted along the surface of Sand 001 top superimposed to show a better view of the high amplitude feature of the identified prospect P1 (Fig.22). High amplitudes were also observed within the vicinity of drilled wells in the area.

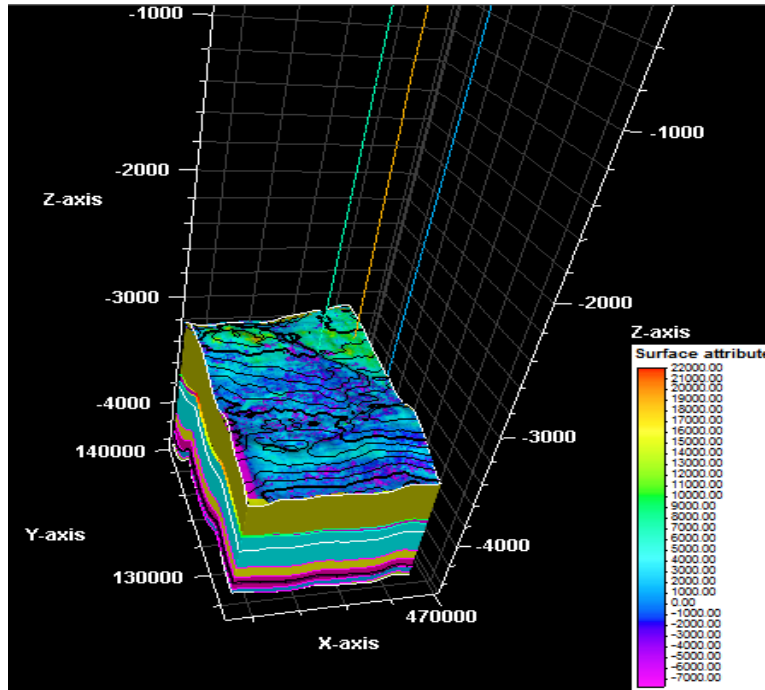


Figure 22. Structural model based on seismic observation in the Bawi field. Maximum amplitude attribute extracted along the surface of Sand 001 top superimposed to show a better view of the amplitude feature of the identified prospect P1. High amplitudes are also observed within the vicinity of drilled wells.

4.5. Petrophysical analysis and volumetric determination

Gross reservoir thickness interval is the interval covering shale and sand within a reservoir. Net thickness of sand is the interval covering only sand within a reservoir. It is called net productive sand. The gross reservoir thickness is determined by knowing interval covering both sand and shale within the reservoir studied using gamma ray log. Net sand thickness is determined by subtracting the interval covering the shale from gross reservoir thickness. Well log data were used in this analysis to generate rock properties using the following formulae: The net-to-gross ratio (*NTG*) is mathematically expressed as:

$$NTG = (NST/GST) \dots \dots \dots (2)$$

where *NST* is the net sand thickness (if shale is present in the formation) while *GST* is gross sand thickness.

Similarly, the gamma ray log was used to calculate the volume of shale in a porous reservoir. The first step used to determine the volume of shale from a gamma ray log was the calculation of the gamma ray index using the equation:

$$I_{GR} = \frac{GR_{log} - GR_{min}}{GR_{max} - GR_{min}} \dots \dots \dots (3)$$

where I_{GR} = gamma ray index, GR_{log} = gamma ray reading of the formation, GR_{min} = minimum gamma ray (clean sand) while GR_{max} = maximum gamma ray (shale). All these values were read off within a particular reservoir. Having obtained the gamma ray index from equation 2 above, volume of shale was then calculated using the Dresser Atlas [42] formula for tertiary consolidated sand given as:

$$V_{sh} = 0.083(2^{3.7 \times I_{GR}} - 1) \dots \dots \dots (4)$$

Another very important rock property is porosity which is defined as the percentage of voids to the total volume of rock. The Formation density log was used to determine formation porosity. The porosity was determined by substituting the bulk density readings obtained from the density log within each reservoir into the equation 4 [42,52].

$$\phi_{den} = \frac{\rho_{ma} - \rho_b}{\rho_b - \rho_f} \dots \dots \dots (5)$$

where, ϕ_{den} is the density derived porosity, ρ_{ma} is the matrix density and is given as 2.65 gm/cm³(for sand/ sandstone), ρ_f is the fluid density which has a value of 1.1gm/cm³ (fluid density) and ρ_b is the formation bulk density.

Determination of the water saturation for the uninvaded zone was achieved using the Archie's (1942) equation:

$$S_w^2 = \frac{F \times R_w}{R_t} \dots \dots \dots (6)$$

$$F = \frac{R_o}{R_w}, S_w^2 = \frac{R_o}{R_t}$$

$$S_w = \sqrt{\frac{R_o}{R_t}} \dots \dots \dots (7)$$

where, S_w = water saturation of the uninvaded zone, R_o = resistivity of formation at 100% water saturation, R_t = true formation resistivity, F = formation factor and R_w = formation water resistivity

4.6. Volumetrics (Reserve estimation) of the "Bawi" Field

Integrating the petrophysical parameters calculated, oil/water contacts determined, and value of recovery factor known, volume of hydrocarbon in place was then computed. The petrophysical parameters deduced from well logs are water saturation (S_w), porosity (ϕ), Net to Gross (NTG) and Volume of Shale (V_{sh}). The tables below summarizes the average results of these important petrophysical parameters utilized as variables for reserve estimation. The volumetric analysis was limited to Hydrocarbon Pore Volume (HCPV) estimation due to non-availability of value for Formation Volume Factor (FVF). Using a recovery factor of 20%, reserve estimate calculated for reservoir R2 gave 795 million barrels; reservoir R4 has a total of 227 million barrels and reservoir R3 has a total of 177 million barrels. Reservoir R1, which is thought to be predominantly gas because of its very high resistivity, contains very little quantity of hydrocarbon (less than a million cubic feet). The total HCPV estimate is about 1.2 billion barrels.

Table 1. Petrophysical evaluation results of the "Bawi" Field

Reservoir sand	Porosity ϕ	Net to gross	V shale	S_w	Sh
Sand 001	0.380	0.878	0.168	0.443	0.557
Sand 002	0.220	0.862	0.097	0.283	0.717
Sand 003	0.205	0.603	0.040	0.315	0.685
Sand 004	0.190	0.665	0.187	0.333	0.667

Table 2. Volumetric estimation results of the Bawi Field

Horizon	Contact	HC Area [*10 ⁶ m ³]	Bulk Volume [*10 ⁶ m ³]	Net Volume [*10 ⁶ m ³]	Pore Volume [*10 ⁶ m ³]	HCPV[*10 ⁶ m ³]
1	2915.00	0.00	0	0	0	0
2	3737.21	77.86	5843	5037	1108	795
3	3975.67	52.24	2086	1258	258	177
4	4129.98	51.86	2696	1793	341	227

4.7. Integrated prospect ranking and risk analysis

In the identified prospects, fault closures form the main hydrocarbon trapping mechanism. In terms of trap integrity, trapped hydrocarbon may be compromised if the faults are non-sealing. The risk is lower where cross-fault juxtaposition is established. Similarly, faults that display growth are commonly sealing, but those without growth may also seal if there is sufficient clay smear, or if reservoir sands are juxtaposed against shales [28]. Prospects of the same closure type but with higher attribute anomaly are ranked higher provided there is no significant difference in estimated volume whereas prospects associated with low volumes are considered to have high risk. A Channel is given a high rank, as channel sands form good stratigraphic traps for hydrocarbon entrapment [43]. Table 3 below is an integrated ranking and risk analysis of identified prospects in "Bawi field".

Table 3. Integrated prospect ranking and risk analyses of Bawi Field

Prospect	Horizon	Attribute Anomaly	Associated volume	Closure Type	Risk	Rank	Remarks
P1	1	Evident	Low	Upthrown/ Footwall Fault closure	High	4	
P3	4	Evident	High	Downthrown/ Hanging Wall Fault closure	Low	3	Fault shows considerable growth
P2	3	Evident	High	Downthrown/ Hanging Wall Fault closure	Low	2	Cross fault juxtaposition observed
Stratigraphic Channel Prospect	2	Evident	High		Low	1	Thickest part of channel targeted

5. Conclusion and recommendation

5.1. Conclusion

This study has demonstrated how a methodology that integrates seismic attributes in seismic interpretation technique can help overcome pitfalls in interpretation and make for a more precise prospect identification and prediction. The trapping elements that were distinguished in the study area include anticlinal dip closures, up thrown fault closures and down thrown fault closures. Growth structures (faults) characterize the structural style in the Oil field. Their complexity increases generally towards the lower section of the delta region. Mapped fault trends were observed to be in the NW-SE direction. The environment of deposition based on wire line logs can be described as a fluvial and "fluvio-deltaic" system. Fining and coarsening upward facie successions were clearly defined. The fluvial system deposited the topmost sand body which is the thickest. The main heterogeneities identified correspond to increasing shaliness in the reservoir due to the environment of deposition. It was deduced that reservoir R2 is the most oil prolific while R1 is the least within the study interval. The total hydrocarbon pore volume (HCPV) in the Oil field is 1.2 billion barrels.

5.2. Recommendation

It is recommended that detailed analysis involving sequence stratigraphy and seismic stratigraphy be incorporated into field studies for better understanding of the stratigraphic plays in the area. Sequence stratigraphic analysis would better define the environment of deposition of the stratigraphic successions, while seismic stratigraphy will better reveal stratigraphic traps in the Oil field. From previous studies, overpressure zones are likely where channels exist in an Oil province like the Niger Delta. Predrill pore-pressure prediction should be carried out to support drilling plan for the stratigraphic channel prospect identified in the Oil field.

Acknowledgement

The authors are sincerely grateful to the management of Total E & P Nigeria Limited and the Department of Petroleum Resources (DPR), Nigeria for their various roles in provision of research data and materials for this work.

References

- [1] Chopra S, and Marfurt KJ. Seismic attributes for prospect identification and reservoir characterization. Society of Exploration Geophysicists geophysical development series 2007, no. 11.
- [2] Chopra S, Pruden D and Alexeev V., 2004. Multi-attribute seismic analysis – tackling non-linearity. *First Break*, 2004; 22(12): 43-47.
- [3] Brown AR Understanding seismic attributes. *Geophysics*, 2001; 66:47– 48.
- [4] Partyka G, Gridley J, and Lopez J. Interpretational applications of spectral decomposition in reservoir characterization; *The Leading Edge*, 1999; 18:353–360, doi:10.1190/1.1438295.
- [5] Burns S, and Street K. Spectral decomposition highlights faults. *Hart's E&P*, March 2005, <http://www.epmag.com/archives/digitalOilField/2135.htm>.
- [6] Castagna JP, Sun S, and Siegfried RW. Instantaneous spectral analysis: detection of low-frequency shadows associated with hydrocarbons. *The Leading Edge*, 2003; 22: 120-127.
- [7] Dorn GA. Modern 3-D seismic interpretation. *The Leading Edge*, 1998; 17(9): 1262–1272
- [8] Jones TA and Helwick SJ. Methods of generating 3-D Geologic models incorporating geologic and geophysical constraints, United States Patent, USOO5838634A., Nov, 1998.
- [9] Gao D. Volume texture extraction for 3-D seismic visualization and interpretation. *Geophysics*, 2003; 68: 1294-1302.
- [10] Gao D. Texture model regression for effective feature discrimination: Application to seismic facies visualization and interpretation. *Geophysics*, 2004; 69: 958- 967.
- [11] Chopra S and Marfurt K. Seismic Attributes – a promising aid for geologic prediction. *CSEG RECORDER*, Special Edition, 2006: 111-121.
- [12] Taner MT, Koehler F, and Sheriff RE. Complex seismic trace analysis. *Geophysics*, 1979; 44: 1041–1063.
- [13] Bahorich M and Farmer S. 3-D seismic discontinuity for faults and stratigraphic features: The coherence cube. *The Leading Edge*, 1995; 14: 1053–1058.
- [14] Marfurt KJ and Kirlin RL. 3-D broad band estimates of reflector dip and amplitude. *Geophysics*, 2000; 65: .304–320.
- [15] Sangree JB, and Widmier JM. Interpretation of depositional facies from seismic data: *Geophysics*, 1979; 44:, 131-160,165–184.
- [16] Love PL, and Simaan M. Segmentation of stacked seismic data by the classification of image texture: 54th Annual International Meeting 1984, SEG, session S7.3.
- [17] Gao D. Latest developments in seismic texture analysis for subsurface structure, facies, and reservoir characterization: A review. *Geophysics*, 2011; 76(2): W1–W13.
- [18] Love PL. and Simaan M. Segmentation of stacked seismic data by the classification of image texture: 54th Annual International Meeting 1984, Society of Exploration Geophysicists, Session:S7.3.
- [19] Vinther R, Mosegaard K, Kierkegaard K, Abatzis I, Andersen C, and If F. Seismic texture classification: A computer-aided approach to stratigraphic analysis. 65th Annual International Meeting 1995, Society of Exploration Geophysicists Expanded Abstracts, 153-155.
- [20] Vinther R. Seismic texture classification applied to processed 2-D and 3-D seismic data. 67th Annual International Meeting 1997, Society of Exploration Geophysicists Expanded Abstracts, 721- 724.
- [21] Whitehead P, Fairborn J, and Wentland R. Identifying stratigraphic units by seismic patterns, 69th Annual International Meeting 1999, Society of Exploration Geophysicists Expanded Abstracts, 942-945.
- [22] West B, May S, Eastwood JE, and Rossen C. Interactive seismic facies classification using textural and neural networks. *The Leading Edge*, 2002; 21:1042-1049.
- [23] Cooke DA and Muryanto T. Reservoir Quantification of B Field, Java Sea via Statistical and Theoretical Methods. Submitted for presentation at the SEG International Exposition and Meeting 1999, Houston, TX USA.
- [24] Evamy DDJ, Haremboure P, Kamerling WA, Knaap F, Molloy A, Rowlands MH. Hydrocarbon habitat of the Tertiary Niger Delta. *American Association of Petroleum Geologists Bulletin*, 1978; 62: 1–39.

- [25] Avbovbo AA.1978. Tertiary lithostratigraphy of Niger Delta. American Association of Petroleum Geologists Bulletin, 1978; 62: 295-300.
- [26] Merki PI. Structural Geology of Cenozoic Niger Delta. First African Regional Geological Conference Proceedings Ibadan University Press 1971, Ibadan, Nigeria; p.251 –266.
- [27] Ejedawe JE. Patterns of incidence of oil reserves in Niger Delta Basin: American Association of Petroleum Geologists, 1981; 65: 1574-1585.
- [28] Doust H and Omatsola E.1990. Niger Delta, in, Edwards JD, and Santogrossi PA, eds., Divergent/passive Margin Basins, AAPG Memoir 48: Tulsa, American Association of Petroleum Geologists, 1990; 239-248.
- [29] Ekweozor CM, Okogun JI, Ekong DEU and Maxwell JR. Preliminary organic geochemical studies of samples from the Niger Delta, Nigeria: Part 1, Analysis of crude oils for triterpanes: Chemical Geology, 1979; 27: 11-28.
- [30] Whiteman AJ. Nigeria: Its Petroleum Geology: Resources and Potential. 1&2. Graham and Trotton: London 1982, UK;p.394.
- [31] Beka FT and Ot, MN. The distal Offshore Niger Delta: frontier prospects of a mature petroleum province, in, Oti, M.N., and Postma, G., eds., Geology of Deltas: Rotterdam 1995, A.A. Balkema; p. 237- 241.
- [32] Bilotti F and Shaw JH, 2005.Deepwater Niger Delta Fold and Thrust Belt modeled as a Critical – Taper Wedge: The Influence of Elevated Basal Fluid Pressure on Structural Styles. AAPG Bulletin, 2005; 89(11): 1475-1491.
- [33] Owoyemi AO and Willis BJ. Depositional Patterns Across Syndepositional Normal Faults, Niger Delta, Nigeria; Journal of Sedimentary Research, 2006; 76: 346-363.
- [34] Weber KJ. 1987.Hydrocarbon distribution patterns in Nigerian growth fault structures controlled by structural style and stratigraphy; Journal of Petroleum Science and Engineering., 1987; 1: 91-104.
- [35] Tuttle MLW, Charpentier RR and Brownfield ME. The Niger Delta Basin Petroleum System: Niger Delta Province, Nigeria, Cameroon, and Equatorial Guinea, Africa; Open- File Report 99-50-H, United States Geological Survey World Energy Report 1999, 44pp.
- [36] Bouvier JD, Kaars-Sijpesteijn CH, Kluesner DF and Onyejekwe CC. 1989. Three- Dimensional Seismic Interpretation and Fault Sealing Investigations”. Nun River Field, Nigeria. AAPG Bulletin., 1989; 73(11): 1397 – 1414.
- [37] Etu-Efeotor JO. Fundamentals of Petroleum Geology. Africana-Fep Publishers, Onitsha 1997, Nigeria, pp: 111-123.
- [38] Stacher P. Present understanding of the Niger Delta hydrocarbon habitat. [In:] M.N. Oti & G. Postma (Eds): Geology of Deltas. Balkema, Rotterdam 1995, 257–268.
- [39] Xiao H and Suppe J.1992. Origin of Rollover. American Association of Petroleum Geologists Bulletin, 1992; 76: 509-229.
- [40] Jolley SJ, Fisher QJ, and Ainsworth RB. 2010. Reservoir compartmentalization: an introduction. Geological Society, London, Special Publications 2010; 347: 1- 8.
- [41] Laughlin K, Garossino P, and Partyka G. Spectral Decomposition for Seismic Stratigraphic Patterns. Online Journal for E&P Geoscientists, 2003.
- [42] Dresser Atlas.,1979. Log interpretation charts Dresser Industries Inc, Houston, Texas, p.107.
- [43] Caldwell J, Chowdhury A, van Bommel, Engelmark F, Sonneland L and Neidell NS. Exploring for stratigraphic traps. Schlumberger Oilfield Review 1997; pp.49-61.
- [44] Eichkitz CG, Schreilechner MG, and Groot PD, and Amtmann J. 2014.Mapping directional variations in seismic character using gray-level co-occurrence matrix-based attributes. Interpretation, 2014; 3(1): T13–T23.
- [45] Xia S, Li Q, Wang X, Sun C, Wang Y, Hu A, Li X and Zheng Q.,2010. Application of 3-D fine seismic interpretation technique in Dawangzhuang Area, Bohai Bay Basin, Northeast China. Arabian Journal of Geosciences, 2010; 1-11, DOI 10.1007/s12517-013-1225-6.
- [46] Abdul Kalid NZ, Hamzah U, and Samsudin AR. Seismic Attributes And Their Application In Faults Interpretation of Kupe Field, Taranaki Basin, New Zealand. EDJE, 2016; 21(6): 2169-2184.
- [47] Kluesner JW and Brothers DS., 2016. Seismic attribute detection of faults and fluid pathways within an active strike-slip shear zone: New insights from high-resolution 3D P-Cable™ seismic data along the Hosgri Fault, offshore California. Interpretation,2016; 4(1): SB131-SB148.
- [48] Castanie L, Bosquet F and Levy B. Advances in seismic interpretation using new volume visualization techniques. First Break, 2005; 23: 69-72.

- [49] Sullivan MD, Jensen GN, Goulding FJ, Jennette DC, and Stern D. 2000. Architectural analysis of deep- water outcrops: Implications for exploration and production of the Diana sub-basin, Western Gulf of Mexico. In: P. Weimer et al. (eds) Deep-Water Reservoirs of the World. GSC-SEPM Foundation 20th Annual Bob F. Perkins Research Conference, pp. 1010-1031.
- [50] Malleswar MR and Marfurt KJ. Seismic texture analysis for reservoir prediction and characterization. *The Leading Edge*, 2010; Special Edition; p.1116-1121.
- [51] Pereira LA. Seismic attributes in hydrocarbon reservoirs characterization. Universidade de Aveiro 2009, p. 1- 183.
- [52] Kendall CG. Template for "conceptual models" used to interpret depositional systems USC Sequence Stratigraphy. <http://strata.geol.sc.edu/index.html>, University of South Carolina.
- [53] Hamed EM and Kurt JM. Structural interpretation of the Middle Frio Formation using 3-D seismic and well logs: An example from the Texas Gulf Coast of the United States. *The Leading Edge*, 2008; 27 (7):840-854.
- [54] Khan HM, Woobaidullah ASM and Quamruzzaman C. 2013. Seismic Interpretation of 2-D Data over Kailashtila Gas Field, NE Bangladesh. *International Journal of Emerging Technology and Advanced Engineering*, 2013; 3(11): 23-34.
- [55] Wiener RW, Helwig JA, and Rongpei J. Seismic Interpretation and Structural Analysis of the Rifted Thrust Belt, Jiangnan Basin, China. *The Leading Edge*, 1997; 60(8): 1177 – 1183.
- [56] Opara AI. Prospectivity Evaluation of "Usso" Field, Onshore Niger Delta Basin, Using 3-D Seismic and Well Log Data. *Pet Coal*, 2010; 52 (4).307-315.
- [57] Mejias M. A Geological Interpretation of 3-D Seismic Data of a Salt Structure and Subsalt Horizons in the Mississippi Canyon, Subdivision of the Gulf of Mexico; University of New Orleans Theses and Dissertations 2006, 438p.
- [58] Reyment RA. Aspects of the geology of Nigeria, university of Ibadan press 1965, Nigeria; 145p.
- [59] Short KC and Stäuble AJ. Outline of geology of Niger Delta: *American Association of Petroleum Geologists Bulletin.*, 1965; 51: 761-779.
- [60] Doust H. The Niger Delta hydrocarbon potential, a major Tertiary Niger Province; *Proceedings of KNGMG Symposium, Coastal Lowstands, Geology and Geotechnology, The Hague, Kluiver Acad. Publ.* 1989, Dordrecht., p.22-25.
- [61] Weber KJ and Daukoru EM. Petroleum geology of the Niger Delta: *Proceedings of the Ninth World Petroleum Congress 1975, volume 2, Geology: London, Applied Science Publishers, Ltd*; p.210-221.
- [62] Castillo F. Seismic Attributes for 3-D Fracture Interpretation; *Geo-Canada 2010 – Working with the Earth 2010*, pp.1-4.
- [63] Posamentier HW, and Allen GP. Siliciclastic sequence stratigraphy - concepts and applications: *SEPM Concepts in Sedimentology and Paleontology*, 2000; 7: 210.
- [64] Serra, O. Sedimentary environments from wireline logs: Houston, Schlumberger 1985, 211 p.
- [65] van Rensbergen P, and Morley CK. 3-D Seismic study of a shale expulsion syncline at the base of the Champion delta, offshore Brunei and its implications for the early structural evolution of large delta systems. *Journal of Marine and Petroleum Geology*, 2000; 17: 861–872.

To whom correspondence should be addressed: Dr. A. I. Opara, Department of Geosciences, Federal University of Technology, PMB 1526, Owerri, Imo State, Nigeria, oparazanda2001@yahoo.com